

Configurational Flexibility of Epimeric β -Aminothioether-chelated Ruthenium(II) η^6 -Arene Complex Salts

Immo Weber^{a,c}, Frank W. Heinemann^a, Walter Bauer^b, and Ulrich Zenneck^a

^a Department Chemie & Pharmazie, Anorganische Chemie, Egerlandstraße 1, Friedrich-Alexander-Universität Erlangen-Nürnberg, D-91058 Erlangen, Germany

^b Department Chemie & Pharmazie, Organische Chemie, Henkestraße 42, Friedrich-Alexander-Universität Erlangen-Nürnberg, D-91054 Erlangen, Germany

^c Present address: Institut für Physikalische Chemie, Technische Universität Bergakademie Freiberg, Leipziger Straße 29, D-09596 Freiberg, Germany

Reprint requests to Prof. Dr. Ulrich Zenneck. Fax: ++49/(0) 9131 8527367.

E-mail: ulrich.zenneck@chemie.uni-erlangen.de

Z. Naturforsch. **2009**, *64b*, 123–140; received November 16, 2008

Dedicated to Professor Otto J. Scherer on the occasion of his 75th birthday

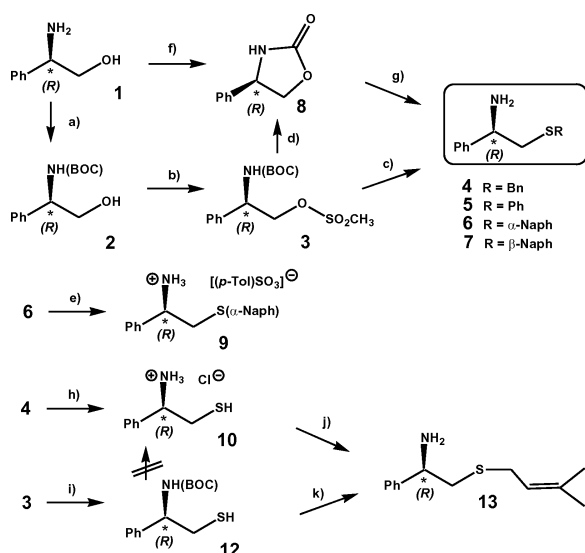
Five chiral β -aminothioethers were obtained *via* different routes orientated on literature protocols. Three of these β -aminothioethers were reacted with two di- μ -chloro-bis{chloro[η^6 -arene]-ruthenium(II)} derivatives, resulting in the title complex salts. The complex cations exhibit three stereocenters, *viz.* ruthenium and sulfur atoms and the chiral benzylic carbon atom of the chelate ligand backbone. Both, ruthenium and sulfur stereocenters epimerize into a mixture of four NMR distinguishable diastereomers in equilibrium, but the designed chiral benzylic carbon atom is stable under all conditions applied so far. The relative diastereomer concentrations in solution depend mainly on the spatial requirements of the η^6 -arene ligand rather than on the thioether moiety. Diastereomer ratios and the absolute configurations in solution were studied by NMR and CD spectroscopy. The spectroscopic results fit to the absolute X-ray crystal structure parameters determined for the diastereomers present in the crystalline state.

Key words: Ruthenium, Arene Complexes, β -Aminothioether Ligands, Stereochemistry, CD Spectroscopy, Epimerization Equilibrium

Introduction

Thioether and thiolato Ru(II) η^6 -arene complexes and the selenium or tellurium analogs thereof are rare [1], but have experienced an increasing interest recently. Mashima prepared bis-thiolato, thiolato and μ -bridged thiolate, selenolate and telluroate Ru(II) η^6 -arene complexes, which exhibit $p\pi$ backbonding from the chalcogenido moiety to the Ru(II) center and a tendency for dimerization unprecedented for Ru(II) η^6 -arene complexes [1a, b]. Chérioux, Süß-Fink, and Therrien extended this class of complexes to dinuclear hydrido clusters [1c–f] which can act as reductive desulfuration reagents. While such chalcogenido complexes are air-sensitive due to enhanced electron density at the Ru(II) center, monodentate thioethers complexed to Ru(II) η^6 -arene fragments are air-stable, but coordinatively labile; nevertheless Ru(II) η^6 -arene complexes bearing monodentate thioether ligands can be isolated [1g]. This coordinative lability can be over-

come if the thioether bears at least one additional donor functionality to form a chelate. Hamaker and co-workers introduced Schiff base ligands with N- and S-donor functionalities to obtain salts with the cations [RuCl(η^6 -arene)(N \cap S)]⁺ which are stable in air and with respect to hydrolysis [1h]. Bennett and Goh placed a Ru(II) η^6 -HMB (= hexamethylbenzene) fragment into a trithio crown ether, which was opened under base-induced fragmentation to a bis-thiolato Ru(II) η^6 -HMB complex in the first step and underwent also base-induced intramolecular Michael cyclization to an *ansa*-thioether Ru(II) η^6 -arene complex [1i–l]. A related observation was made by Teixidor and Hursthouse for thioether η^6 -arene Ru(II) carborane complexes [1m], and some complexes of this class react also with alkynes [1n]. Successful applications of chiral thioether complexes in enantioselective catalysis are rare [2a–g]. An inherent problem is the control of the configurational stability of the coordinated sulfur atom. Inversion barriers of $\Delta G^\ddagger_{298} = 41–49$ kJ mol⁻¹



Scheme 1. Preparation of chiral β -aminothioethers **4–7**; a) see ref. [6b]; b) MeSO₂Cl (1.23 equiv.), Et₃N (1.51 equiv.), CH₂Cl₂, 0 °C to r.t.; c) 1–2.2 equiv. RSK; THF, MeOH as indicated in the Exp. Section; work-up with 36 % HCl; d) up to 20 % formation of **8** in a side reaction of path c; e) (*p*-Tol)SO₃H·(H₂O) (1.01 equiv.), EtOH, recrystallization; f) see ref. [7a–b]; g) Ishibashi protocol for **4**, **5** and **7** (1.3–2.9 equiv. RSH / 2.2–4.9 equiv. RSNa / 12–24 h reflux in *n*-PrOH); h) 1. Na (4.88 equiv.), ^tBuOH (1.26 equiv.), liquid NH₃, THF, –78 °C; 2. excess NH₄Cl; 3. EtOH, 36 % HCl; i) 1. KSAc (1.49 equiv.), MeOH, THF; 2. excess gas. NH₃, all r.t.; j) 1. ^tBuOK (1.81 equiv.), MeOH; 2. PrenylBr (1.12 equiv.); 3. 36 % HCl, all r.t.; k) 1. ^tBuOK (1.10 equiv.), THF; 2. PrenylBr (1.19 equiv.); 3. 36 % HCl, all r.t.

for Pt(IV) [2h] and of $\Delta G^\ddagger_{298} = 51–56$ kJ mol^{–1} for Cr(0)(CO)₅ thioether complexes were found [2i]. Low inversion barriers of the coordinated sulfur atoms were also observed for simple pyridyl- and pyrimidyl-thioether Ru(II) complexes [2j].

The factors controlling the inversion barriers of Ru(II)-coordinated thioethers is addressed in the work presented here by complexing various chiral β -amino thioether ligands on two Ru(II) η^6 -arene fragments. The intention was to address the question whether it is possible to transfer the concept of Noyori [3a–i] for enantioselective ruthenium transfer hydrogenation catalysts from chiral β -aminoalcohol chelate ligands to their β -aminothioether analogs. Although configurational stability is not always a requirement for a highly enantioselective transfer hydrogenation catalyst as shown by Pfeiffer [3j], the understanding of configurational stability of chiral Ru(II) centers containing η^6 -arene ligands is a major goal of our ongoing work [4].

Table 1. Selected bond lengths (Å) and angles (deg) of the hydrogen *p*-tosylate salt **9**.

Distances		Angles	
N(1)–C(7)	1.502(3)	N(1)–C(7)–C(8)	108.4(2)
S(1)–C(8)	1.806(2)	N(1)–C(7)–C(6)	120.8(2)
S(1)–C(9)	1.776(3)	C(7)–C(8)–S(1)	112.0(2)
C(7)–C(8)	1.525(3)	C(6)–C(7)–C(8)	113.0(2)
C(6)–C(7)	1.516(3)	C(8)–S(1)–C(9)	102.8(2)
S(2)–O(1)	1.441(2)	O(1)–S(2)–O(2)	113.4(2)
S(2)–O(2)	1.459(2)	O(1)–S(2)–O(3)	133.3(2)
S(2)–O(3)	1.461(2)	O(2)–S(2)–O(3)	110.5(2)
S(2)–C(19)	1.779(2)	O(3)–S(2)–C(19)	106.1(1)

Table 2. Interionic hydrogen bonds (Å, deg) in the hydrogen *p*-tosylate salt **9**.

D–H...A	<i>d</i> (D–H)	<i>d</i> (H...A)	<i>d</i> (D...A)	\angle (D–H...A)
N(1)–H(1A)...O(3)	0.91	1.87	2.769(3)	171.4
N(1)–H(1B)...O(2) ^a	0.91	2.01	2.834(3)	149.3
N(1)–H(1B)...O(1) ^b	0.91	2.36	2.930(3)	120.2
N(1)–H(1C)...O(3) ^c	0.91	2.29	3.180(3)	167.0
N(1)–H(1C)...O(2) ^c	0.91	2.36	3.008(3)	127.7

Symmetry transformations: ^a $-x+1, y-1, -z+1$; ^b $-x+1, y, -z+1$; ^c $x, y-1, z$.

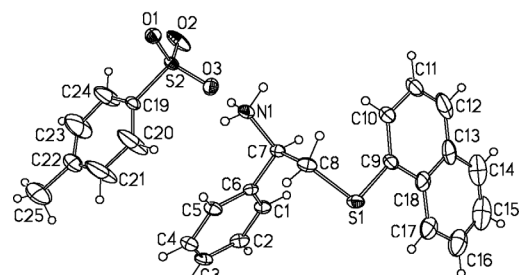
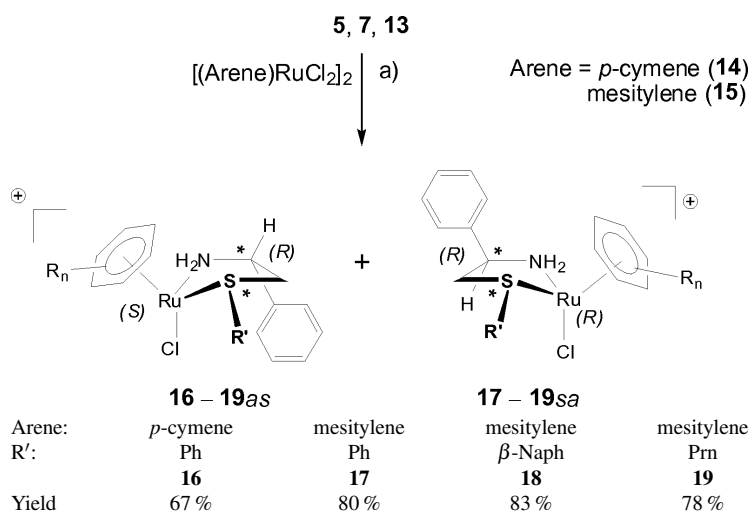


Fig. 1. Displacement ellipsoid plot (50 % probability) of the molecular structure of hydrogen *p*-tosylate salt **9**. For selected intraionic distances and angles see Table 1; interionic hydrogen bonds are listed in Table 2.

Results and Discussion

Syntheses of the chiral β -amino thioether ligands

β -Amino sulfides are versatile intermediates in organic synthesis [5a–i]. They are important as building blocks of biologically active compounds [5j–n]. (*R*)-Phenyl-glycinol (**1**) [6a] was converted into the mesylate **3** in high yield and sufficient purity for further reactions without work-up [2h, 6b] via the BOC protected (*R*)- β -amino alcohol **2** (Scheme 1). **3** was reacted then with 1.0–2.2 equiv. of various thiolates at ambient temperature, and the resulting BOC derivatives were deprotected *in situ* with aqueous HCl to form the β -aminothioethers **4–7**. The formation of **5** and **7** was accompanied by the formation of up to 20 % (4*R*)-4-phenyl-2-



Scheme 2. Preparation of (β -aminothioether)(η^6 -arene)Ru(II) complex cations **16–19**; a) 1. **5, 7, 13** (> 2 equiv.), MeOH, r. t.; 2. excess NaPF₆.

oxazolidinone **8** as a by-product, which was difficult to remove.

Raw product **4** was sufficiently pure again for the next step, and crude **6** contained only traces of **8**. Protonation of β -aminothioether **6** by *p*-tosic acid led to ammonium *p*-tosylate salt **9** whose (*R*) configuration was confirmed by X-ray crystal structure analysis (Fig. 1, Table 1).

The ethyl group of the β -ammonium thioether cation of **9** adopts an antiperiplanar conformation in the solid state. Slightly shortened C(7)–C(8) and elongated C(7)–N(1) bonds might indicate a weak σ – σ^* effect [6a–d], but crystal packing and/or hydrogen bonding between the *p*-tosylate and the ammonium group may also affect the details of the molecular structure of **9** in the solid state (Table 2). To circumvent the detrimental by-product formation, this disadvantage was taken as an opportunity to use **8** itself as an aziridine equivalent for the preparation of β -aminothioethers. For that purpose, **1** was converted to **8** [7a–b], and then the Ishibashi protocol [7c–d] was applied for the syntheses of **4**, **5** and **7**. This reaction requires an excess of thiol and thiolate. The yields of the Ishibashi reaction are only high for **4** and **5**, because a moderately volatile thiol is optimal in that case. Vapor pressure of the thiol is not the only issue for a successful application of this reaction sequence as we learned from an unsuccessful attempt to prepare an isopropyl thioether in this way.

With the aim of getting access to β -amino prenylthioether **13**, intermediate **10** was obtained by debenzoylation of **4** following Mellor's protocol [7e] with the

hydrochloride salt, because the free base **11** is considerably sensitive towards oxidation to form the corresponding disulfide. The analogous *in situ* reaction of **3** with potassium thioacetate [7e–g] followed by aminolysis of the acetyl group gave the BOC-protected β -amino thiol **12** only in 40 % yield. The nucleophilic substitution reaction with thioacetate proceeded with good selectivity (TLC), but **8** was observed again in considerable amounts during the aminolysis step. Attempted BOC deprotection of **12** to yield **10** resulted only in quantitative formation of **8** instead, although analogous BOC-deprotection is reported for (*R*)-valinthiol [2g]. *In situ* deprotonation of **10** or **12** with *t*-BuOK followed by allylation lead to clean formation of the desired β -amino prenylthioether **13** in high yields with only trace impurities. Attempted chromatographic purification of **13** reduced the yield significantly. The product is thermosensitive and cannot be distilled.

Syntheses and crystallographic study of the diastereomeric β -aminothioether-chelated Ru(II) η^6 -arene complex salts

Ligands **5–7** reacted smoothly with the Ru(II) η^6 -cymene and η^6 -mesitylene complex dimers **14** [8a, b] and **15** [8a] in all combinations with excess NaPF₆ in MeOH to yield $\sigma(N) : \sigma(S)$ β -aminothioether η^6 -arene Ru(II) chelate complex PF₆ salts. However, only the combinations **14–5**, **15–5**, and **15–7** gave crystalline salts with the cations **16–18** (Scheme 2) which could be characterized by X-ray crystal structure analysis (Figs. 2–4). Only *as* η^6 -ligand *anti* (*a*) and *R'* *syn*

Table 3. Selected bond lengths (Å) and angles (deg) of the complex cation **16** (only the diastereomer **16as** present in the crystal of [**16**][PF₆] examined).

Distances		Angles	
Ru(1)–Cl(1)	2.392(2)	Cl(1)–Ru(1)–S(1)	90.40(4)
Ru(1)–S(1)	2.369(2)	Cl(1)–Ru(1)–N(1)	82.4(1)
Ru(1)–N(1)	2.129(4)	S(1)–Ru(1)–N(1)	82.2(1)
Ru(1)–C(1)	2.200(4)	S(1)–Ru(1)–C(6)	159.0(2)
Ru(1)–C(2)	2.193(4)	S(1)–Ru(1)–C(1)	153.2(2)
Ru(1)–C(3)	2.229(4)	N(1)–Ru(1)–C(4)	157.3(2)
Ru(1)–C(4)	2.197(5)	N(1)–Ru(1)–C(5)	156.2(2)
Ru(1)–C(5)	2.189(4)	Cl(1)–Ru(1)–C(3)	157.8(2)
Ru(1)–C(6)	2.239(5)	Cl(1)–Ru(1)–C(2)	153.4(2)
N(1)–C(11)	1.511(5)	C(19)–S(1)–C(12)	117.1(2)
S(1)–C(12)	1.827(4)	S(1)–C(12)–C(11)	106.0(3)
C(11)–C(12)	1.522(6)	C(12)–C(11)–N(1)	108.2(3)
C(11)–C(13)	1.513(6)	C(12)–C(11)–C(13)	112.9(3)
S(1)–C(19)	1.799(4)	Ru(1)–S(1)–C(12)	99.5(2)
		Ru(1)–N(1)–C(11)	115.3(3)

Table 4. Selected bond lengths (Å) and angles (deg) of complex cation **17as**.

Distances		Angles	
Ru(2)–Cl(2)	2.407(1)	Cl(2)–Ru(2)–S(2)	88.53(4)
Ru(2)–S(2)	2.373(1)	Cl(2)–Ru(2)–N(2)	83.07(9)
Ru(2)–N(2)	2.144(3)	S(2)–Ru(2)–N(2)	81.45(9)
Ru(2)–C(25)	2.193(4)	S(2)–Ru(2)–C(25)	167.8(2)
Ru(2)–C(26)	2.225(4)	S(2)–Ru(2)–C(30)	142.2(2)
Ru(2)–C(27)	2.226(4)	N(2)–Ru(2)–C(26)	145.9(2)
Ru(2)–C(28)	2.198(4)	N(2)–Ru(2)–C(27)	165.5(2)
Ru(2)–C(29)	2.202(4)	Cl(2)–Ru(2)–C(28)	146.9(2)
Ru(2)–C(30)	2.223(4)	Cl(2)–Ru(2)–C(29)	164.4(2)
N(2)–C(35)	1.504(5)	C(43)–S(2)–C(36)	101.5(2)
S(2)–C(36)	1.814(4)	S(2)–C(36)–C(35)	107.1(3)
C(35)–C(37)	1.523(5)	C(36)–C(35)–N(2)	108.0(3)
C(35)–C(37)	1.512(5)	C(36)–C(35)–C(37)	113.9(3)
S(2)–C(43)	1.793(4)	Ru(2)–S(2)–C(36)	99.3(2)
		Ru(2)–N(2)–C(35)	117.0(2)

Table 5. Selected bond lengths (Å) and angles (deg) of complex cation **17sa**.

Distances		Angles	
Ru(1)–Cl(1)	2.400(1)	Cl(1)–Ru(1)–S(1)	91.43(3)
Ru(1)–S(1)	2.400(2)	Cl(1)–Ru(1)–N(1)	83.26(8)
Ru(1)–N(1)	2.148(3)	S(1)–Ru(1)–N(1)	81.42(9)
Ru(1)–C(1)	2.190(4)	S(1)–Ru(1)–C(1)	168.1(2)
Ru(1)–C(2)	2.240(4)	S(1)–Ru(1)–C(6)	135.4(2)
Ru(1)–C(3)	2.216(4)	N(1)–Ru(1)–C(2)	140.5(2)
Ru(1)–C(4)	2.203(4)	N(1)–Ru(1)–C(3)	169.3(2)
Ru(1)–C(5)	2.199(4)	Cl(1)–Ru(1)–C(4)	141.2(2)
Ru(1)–C(6)	2.203(4)	Cl(1)–Ru(1)–C(5)	166.1(2)
N(1)–C(11)	1.491(5)	C(19)–S(1)–C(12)	105.6(2)
S(1)–C(12)	1.824(4)	S(1)–C(12)–C(11)	110.2(3)
C(11)–C(12)	1.533(5)	C(12)–C(11)–N(1)	106.9(3)
C(11)–C(13)	1.526(5)	C(12)–C(11)–C(13)	111.5(3)
S(1)–C(19)	1.784(4)	Ru(1)–S(1)–C(12)	100.3(2)
		Ru(1)–N(1)–C(11)	114.9(2)

(s) and *sa* η^6 -ligand *syn* (s) and *R'* *anti* (a) diastereomers were found in the solid state.

Table 6. Selected bond lengths (Å) and angles (deg) of complex cation **18as**.

Distances		Angles	
Ru(2)–Cl(2)	2.398(2)	Cl(2)–Ru(2)–S(2)	88.97(6)
Ru(2)–S(2)	2.386(2)	Cl(2)–Ru(2)–N(2)	81.0(2)
Ru(2)–N(2)	2.145(5)	S(2)–Ru(2)–N(2)	81.5(2)
Ru(2)–C(31)	2.180(6)	S(2)–Ru(2)–C(35)	165.7(2)
Ru(2)–C(32)	2.198(7)	S(2)–Ru(2)–C(36)	146.6(2)
Ru(2)–C(33)	2.206(6)	N(2)–Ru(2)–C(33)	164.7(2)
Ru(2)–C(34)	2.206(6)	N(2)–Ru(2)–C(34)	148.6(2)
Ru(2)–C(35)	2.188(6)	Cl(2)–Ru(2)–C(31)	159.8(2)
Ru(2)–C(36)	2.231(6)	Cl(2)–Ru(2)–C(32)	151.1(2)
N(2)–C(41)	1.507(6)	C(49)–S(2)–C(42)	100.4(3)
S(2)–C(42)	1.819(5)	S(2)–C(42)–C(41)	108.8(3)
C(41)–C(42)	1.521(6)	C(42)–C(41)–N(2)	109.1(4)
C(41)–C(43)	1.514(7)	C(42)–C(41)–C(43)	109.2(4)
S(2)–C(49)	1.798(6)	Ru(2)–S(2)–C(42)	98.3(2)
		Ru(2)–N(2)–C(41)	118.7(3)

Table 7. Selected bond lengths (Å) and angles (deg) of complex cation **18sa**.

Distances		Angles	
Ru(1)–Cl(1)	2.398(2)	Cl(1)–Ru(1)–S(1)	93.64(6)
Ru(1)–S(1)	2.382(2)	Cl(1)–Ru(1)–N(1)	81.1(2)
Ru(1)–N(1)	2.181(5)	S(1)–Ru(1)–N(1)	81.2(2)
Ru(1)–C(1)	2.209(6)	S(1)–Ru(1)–C(1)	164.5(2)
Ru(1)–C(2)	2.234(6)	S(1)–Ru(1)–C(6)	144.3(2)
Ru(1)–C(3)	2.225(7)	N(1)–Ru(1)–C(2)	149.5(2)
Ru(1)–C(4)	2.230(7)	N(1)–Ru(1)–C(3)	166.7(2)
Ru(1)–C(5)	2.210(6)	Cl(1)–Ru(1)–C(4)	150.2(2)
Ru(1)–C(6)	2.232(6)	Cl(1)–Ru(1)–C(5)	158.3(2)
N(1)–C(11)	1.478(6)	C(19)–S(1)–C(12)	106.3(3)
S(1)–C(12)	1.829(5)	S(1)–C(12)–C(11)	110.4(3)
C(11)–C(12)	1.516(6)	C(12)–C(11)–N(1)	107.6(4)
C(11)–C(13)	1.528(7)	C(12)–C(11)–C(13)	114.6(4)
S(1)–C(19)	1.808(6)	Ru(1)–S(1)–C(12)	100.8(2)
		Ru(1)–N(1)–C(11)	112.7(3)

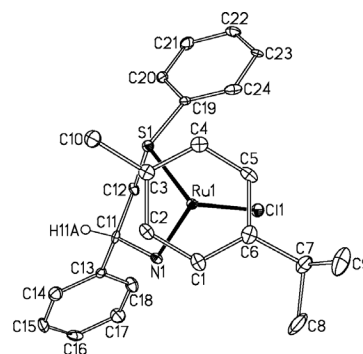


Fig. 2. Displacement ellipsoid plot (50% probability) of the molecular structure of the η^6 -(*p*-cymene) complex cation **16**. Hydrogen atoms (except H11A), PF₆[−], MeOH and CH₂Cl₂ have been omitted for clarity; only diastereomer **16as** is present in the crystal of [**16**][PF₆] examined; for selected bond lengths and angles see Table 3.

Attempts to react **14** and **15** with **11** (obtained by *in situ* deprotonation of **10**) to yield the correspond-

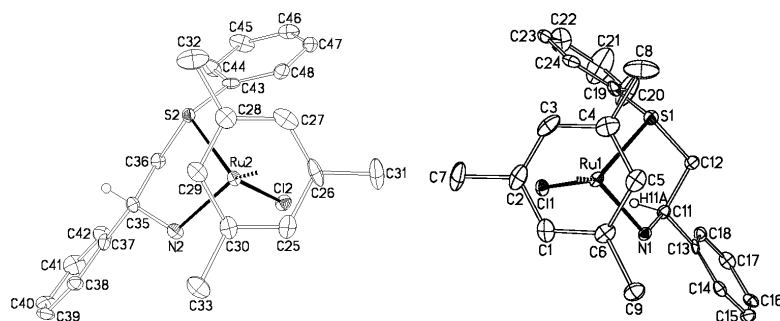


Fig. 3. Displacement ellipsoid plot (50% probability) of the molecular structures of the diastereomeric η^6 -mesitylene complex cations **17as** (left) and **17sa** (right) observed in the unit cell of complex salt [**17**][PF₆]. Hydrogen atoms except H35A and H11A have been omitted for clarity; for selected bond lengths and angles **17as** and **17sa** see Tables 4 and 5, respectively.

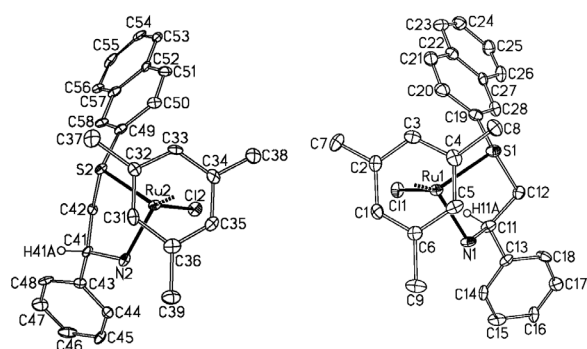


Fig. 4. Displacement ellipsoid plot (50% probability) of the molecular structures of the diastereomeric η^6 -mesitylene complex cations **18as** (left) and **18sa** (right) observed in the unit cell of the complex salt [**18**][PF₆]. Hydrogen atoms except H41A and H11A have been omitted for clarity; for selected bond lengths and angles for **18as** and **18sa** see Tables 6 and 7, respectively.

ing β -aminothiolato η^6 -arene Ru(II) complexes resulted only in product mixtures. To relate the reactivity of **10** or **11** as potential thiolate precursors to an alternative starting material, the prenyl functionality of **13** was introduced as a designed leaving group. However, the η^6 -mesitylene complex dimer **15** reacted with **13** to form the $\sigma(N) : \sigma(S)$ β -amino prenyl thioether η^6 -arene Ru(II) complex cation **19**, which could also be characterized by X-ray crystal structure analysis (Fig. 5). Any attempt to convert **19** *via* allyl-conjugative fragmentation to the desired thiolato complex resulted also in mixtures of several compounds. Comparable fragmentations were achieved by Bennett and Goh [1g–j] and by van der Zeijden with even more electron rich Ru(II) η^5 -Cp complexes [8c]. Compounds **16**–**19** are air-stable in the solid state and in solution. Of all crystals examined, the η^6 -(*p*-cymene) species **16** crystallized always as the pure diastereomer salt [**16as**][PF₆], whereas the η^6 -(mesitylene) complex cations **17**–**19** formed 1 : 1 diastereomeric mixtures of

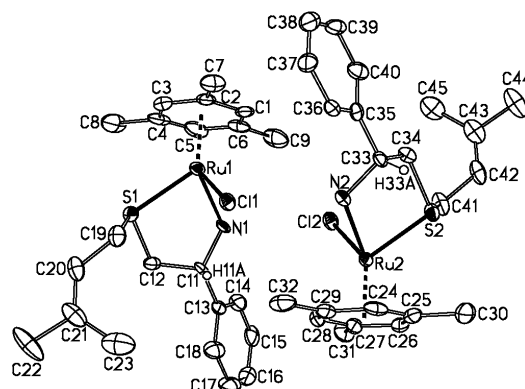


Fig. 5. Displacement ellipsoid plot (50% probability) of the molecular structures of the diastereomeric η^6 -mesitylene complex cations **19sa** (left) and **19as** (right) as observed in the unit cell of the complex salt [**19**][PF₆]. Hydrogen atoms (except H11A and H33A), PF₆[−] and CH₂Cl₂ have been omitted for clarity; selected bond lengths and angles are listed in Tables 8 and 9, respectively.

the *as* and the *sa* diastereomers in the unit cells of their PF₆ salts.

The stereochemical descriptors of the absolute configuration of the chiral Ru(II) centers used in this paper follow the recommendations of Bünzli-Trepp [9] with the results: **16as**–**18as** (*S*_{Ru}, *R*_S, *R*) η^6 -ligand *anti* (*a*) and *R'* *syn* (*s*) in regard to benzylic Ph; **16sa**–**18sa** (*R*_{Ru}, *S*_S, *R*); **16aa**–**18aa** (*S*_{Ru}, *S*_S, *R*); **16ss**–**18ss** (*R*_{Ru}, *R*_S, *R*). Note that for *R'* = Prn the absolute configuration of the chiral sulfur center formally changes: **19as** (*S*_{Ru}, *S*_S, *R*); **19sa** (*R*_{Ru}, *R*_S, *R*); **19aa** (*S*_{Ru}, *R*_S, *R*); **19ss** (*R*_{Ru}, *S*_S, *R*).

As expected from the synthetic route applied, the absolute configuration of the chiral benzylic center of the ligand backbone was confirmed to be (*R*) in all cases. Beyond the molecular details of the ruthenium complex cations in the crystalline state, hydrogen bridging between the coordinated amino groups and the PF₆[−] counteranions is observed for all four salts examined.

Table 8. Selected bond lengths (Å) and angles (deg) of complex cation **19as**.

Distances		Angles	
Ru(2)–Cl(2)	2.409(2)	Cl(2)–Ru(2)–S(2)	88.35(5)
Ru(2)–S(2)	2.364(2)	Cl(2)–Ru(2)–N(2)	83.8(2)
Ru(2)–N(2)	2.147(4)	S(2)–Ru(2)–N(2)	81.7(2)
Ru(2)–C(24)	2.182(6)	S(2)–Ru(2)–C(28)	162.7(2)
Ru(2)–C(25)	2.193(5)	S(2)–Ru(2)–C(29)	148.5(2)
Ru(2)–C(26)	2.202(5)	N(2)–Ru(2)–C(26)	161.0(2)
Ru(2)–C(27)	2.220(5)	N(2)–Ru(2)–C(27)	152.8(2)
Ru(2)–C(28)	2.196(5)	Cl(2)–Ru(2)–C(24)	160.1(2)
Ru(2)–C(29)	2.230(6)	Cl(2)–Ru(2)–C(25)	152.0(2)
N(2)–C(33)	1.509(6)	C(41)–S(2)–C(34)	100.5(3)
S(2)–C(34)	1.836(5)	S(2)–C(34)–C(33)	107.6(3)
C(33)–C(34)	1.490(7)	C(34)–C(33)–N(2)	108.0(4)
C(33)–C(35)	1.512(7)	C(34)–C(33)–C(35)	113.9(4)
S(2)–C(41)	1.836(6)	Ru(2)–S(2)–C(34)	98.8(2)
C(41)–C(42)	1.492(8)	Ru(2)–N(2)–C(33)	116.6(3)
C(42)–C(43)	1.310(10)	C(41)–S(2)–C(34)	100.5(3)
C(43)–C(44)	1.526(9)	S(2)–C(41)–C(42)	109.4(4)
C(43)–C(45)	1.492(10)	C(41)–S(2)–Ru(2)	112.7(2)
		C(41)–C(42)–C(43)	126.5(6)
		C(42)–C(43)–C(44)	120.6(6)
		C(42)–C(43)–C(45)	126.1(6)
		C(44)–C(43)–C(45)	113.3(6)

Table 9. Selected bond lengths (Å) and angles (deg) of complex cation **19sa**.

Distances		Angles	
Ru(1)–Cl(1)	2.399(2)	Cl(1)–Ru(1)–S(1)	91.88(5)
Ru(1)–S(1)	2.390(2)	Cl(1)–Ru(1)–N(1)	84.1(2)
Ru(1)–N(1)	2.127(4)	S(1)–Ru(1)–N(1)	81.8(2)
Ru(1)–C(1)	2.203(6)	S(1)–Ru(1)–C(1)	163.5(2)
Ru(1)–C(2)	2.210(5)	S(1)–Ru(1)–C(6)	146.1(2)
Ru(1)–C(3)	2.180(6)	N(1)–Ru(1)–C(2)	151.3(2)
Ru(1)–C(4)	2.189(6)	N(1)–Ru(1)–C(3)	162.6(2)
Ru(1)–C(5)	2.191(7)	Cl(1)–Ru(1)–C(4)	151.3(2)
Ru(1)–C(6)	2.237(6)	Cl(1)–Ru(1)–C(5)	158.3(2)
N(1)–C(11)	1.493(6)	C(19)–S(1)–C(12)	101.9(3)
S(1)–C(12)	1.821(5)	S(1)–C(12)–C(11)	110.6(3)
C(11)–C(12)	1.526(6)	C(12)–C(11)–N(1)	107.8(4)
C(11)–C(13)	1.521(7)	C(12)–C(11)–C(13)	111.5(4)
S(1)–C(19)	1.839(6)	Ru(1)–S(1)–C(12)	100.5(2)
C(19)–C(20)	1.472(8)	Ru(1)–N(1)–C(11)	115.3(3)
C(20)–C(21)	1.315(9)	C(19)–S(1)–C(12)	101.9(3)
C(21)–C(22)	1.501(9)	S(1)–C(19)–C(20)	111.7(4)
C(21)–C(23)	1.517(11)	C(19)–S(1)–Ru(1)	110.4(2)
		C(19)–C(20)–C(21)	128.9(6)
		C(20)–C(21)–C(22)	122.7(7)
		C(20)–C(21)–C(23)	123.0(6)
		C(22)–C(21)–C(23)	114.2(7)

In addition, [**16**][PF₆] and [**19**][PF₆] incorporate solvent molecules in defined stoichiometric ratios into their crystal structures, which were also confirmed by elemental analysis. This and the repetition of structural motifs in the crystals examined justify the assumption of an inherent preference of the diastereomers observed in the solid state.

Table 10. Averaged angles (deg) $\phi_{trans} = X\text{-Ru(II)-C(i)}(\eta^6\text{-arene})$ (X = N, S, Cl) of all particular diastereomeric η^6 -arene complex cations **16–19** as an indicator of the *trans* influence.

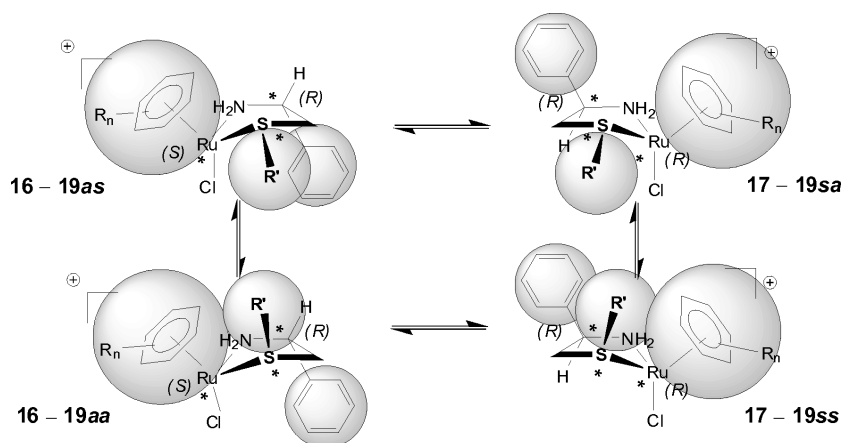
Complex	ϕ_{trans} S	ϕ_{trans} N	ϕ_{trans} Cl
16	156.1	156.8	155.6
17	153.3	155.3	154.6
18	155.3	157.4	154.9
19	155.2	157.0	155.4

All bond lengths and angles are in the expected range. An elongation of the *S*–CH₂ and a shortening of the allyl (–CH₂–CH=C) bond lengths of **19as** and **19sa** are indicative of a potentially labile prenyl group. Although the *S*–CH₂ bonds of **19as** and **19sa** are arranged almost parallel to the alkene π -bonding planes, the small variations of the bond lengths indicate only a very weak stereoelectronic effect [6c–d] in the sense of a $\sigma^*-\pi^*-\sigma$ delocalization, which might be influenced by crystal packing as well (Fig. 5, Tables 8, 9). The C–N and C–S bonds are only slightly elongated. The average Ru–S bond length of 2.38 Å compares well to the ones of phosphine Ru(II)- η^6 -arene complexes. Comparison of the bond angles $\phi_{trans} = X\text{-Ru(II)-C(i)}(\eta^6\text{-arene})$ (X = N, S, Cl) greater or equal 150° reveal slight *trans* influences, but without general tendencies (Table 10). Generally, thioethers are much weaker σ donor and π acceptor ligands than phosphines, and this general effect cannot be significantly influenced or modulated by variation of the sulfur substituent R'.

It is remarkable that we found *as* and *sa* diastereomers with a 1 : 1 ratio in the unit cells of the PF₆ salts of the η^6 -mesitylene cations **17–19**, whereas the only other example with an alternative arene ligand, the η^6 -(*p*-cymene) species **16**, forms a defined crystalline phase with a single *as* diastereomer only. If we assume an increased molecular fragment volume for the (η^6 -*p*-cymene)Ru moiety as compared to (η^6 -mesitylene)Ru, this finding for the crystalline state seems to fit to the CD and NMR spectroscopic results of the compounds in solution, which point to a more pronounced interaction between the five-membered chelate ring substituents and the *p*-cymene ligand (*vide infra*).

CD and NMR studies of diastereomeric β -aminothioether-chelated η^6 -arene complex cations in solution

If steric repulsion with respect to the η^6 -arene ligand is regarded as the dominating factor for the energetic preference of one or two particular diastereomers



Scheme 3. Diastereomer equilibria of the complex cations **16**–**19** in solution; for numbering see Scheme 2.

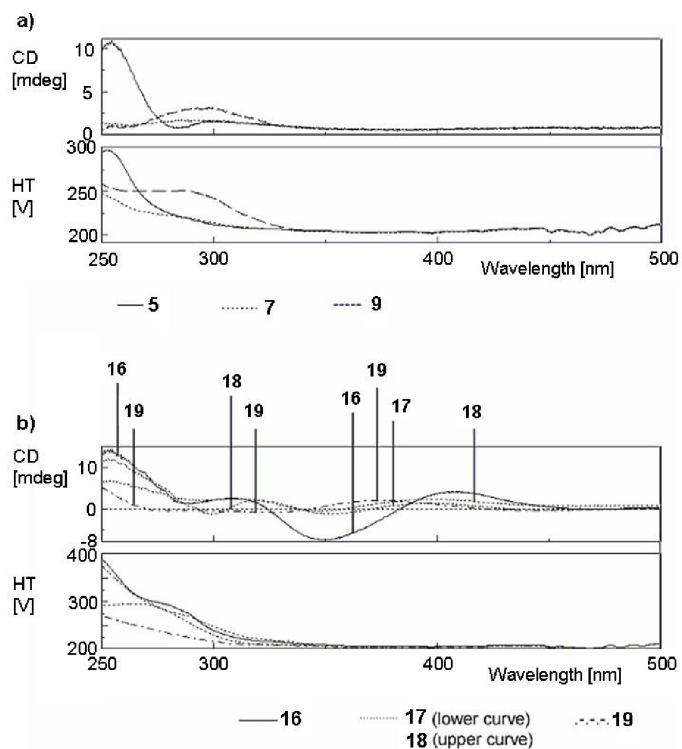


Fig. 6. CD spectra (MeOH, ambient temperature, $c \sim 10^{-6}$ M); a) β -aminothioether derivatives **5**, **7** and **9**; b) β -aminothioether-chelated ruthenium(II) η^6 -arene cations **16**–**19**.

over the four possible (*as*, *aa*, *sa*, *ss*), then the energetic preference should decrease in the general order $as > sa \geq aa > ss$. This consideration is unambiguously clear for the most preferred *as* and the most discriminated *ss* diastereomers, but the relation between *sa* and *ss* diastereomers is not that easily evaluated on a qualitative level. Generally, the *sa* cases should be slightly lower in energy than the *aa* diastereomers as they minimize the axial repulsion between *anti*-

oriented (arene)Ru and SR' moieties, which are *syn*-oriented for the *aa* diastereomers (Scheme 3).

A close match of the CD spectra of complex cations **16**–**19** and free β -aminothioether ligands **5**, **7** and **9** in the range 250–300 nm (Fig. 6) are indicative of small contributions of both, the coordinated ruthenium metal and the sulfur atom stereocenters to the chiroptical properties in that spectral range of the asymmetric compounds. An equilibrium of diastere-

Table 11. Crystallographic data of **9**, [**16**][PF₆]·(CH₂Cl₂)_{0.5}·(MeOH), [**17**][PF₆], [**18**][PF₆], and [**19**][PF₆]·(CH₂Cl₂)_{0.5}.

	9	[16][PF ₆](CH ₂ Cl ₂) _{0.5} ·(MeOH)	[17][PF ₆]	[18][PF ₆]	[19][PF ₆](CH ₂ Cl ₂) _{0.5}
Emp. formula	C ₂₅ H ₂₅ NO ₃ S ₂	C _{25.5} H ₃₄ Cl ₂ F ₆ NOPRuS	C ₂₃ H ₂₇ ClF ₆ NPRuS	C ₂₇ H ₂₉ ClF ₆ NPRuS	C _{22.5} H ₃₂ Cl ₂ F ₆ NPRuS
Mol. weight	451.58	719.54	631.01	681.06	665.49
Color, shape	colorless, needle	yellow, platelet	yellow, block	orange, block	yellow, block
Crystal size, mm ³	0.35 × 0.10 × 0.08	0.37 × 0.24 × 0.05	0.16 × 0.13 × 0.07	0.21 × 0.14 × 0.12	0.18 × 0.18 × 0.16
<i>T</i> , K	100	100	100	100	100
Crystal system	monoclinic	monoclinic	monoclinic	monoclinic	monoclinic
Space group	C2 (no. 5)	C2 (no. 5)	<i>P</i> 2 ₁ (no. 4)	<i>P</i> 2 ₁ (no. 4)	C2 (no. 5)
<i>a</i> , Å	28.108(3)	19.170(2)	10.1658(7)	10.229(1)	15.934(2)
<i>b</i> , Å	5.2575(3)	8.8851(5)	12.3733(5)	10.759(1)	15.537(2)
<i>c</i> , Å	15.758(2)	17.328(2)	20.161(1)	24.477(2)	23.330(3)
β , deg	102.052(6)	97.250(9)	90.670(6)	93.626(6)	104.67(2)
<i>V</i> , Å ³	2277.4(4)	2927.8(5)	2535.8(2)	2688.4(4)	5587(2)
<i>Z</i>	4	4	4	4	8
ρ , g cm ⁻³ (calc.)	1.317	1.632	1.653	1.683	1.582
μ , mm ⁻¹	0.261	0.904	0.926	0.880	0.937
<i>F</i> (000), e	952	1460	1272	1376	2696
Abs. corr.	multiple scans	numerical	multiple scans	numerical	multiple scans
Abs. corr.	(SADABS)	(Gauss integration)	(SADABS)	(Gauss integration)	(SADABS)
<i>T</i> _{min} ; <i>T</i> _{max}	0.906; 0.980	0.801; 0.965	0.813; 0.940	0.844; 0.905	0.740; 0.860
2 θ range, deg	6.5–54.2	5.7–56.0	6.8–54.2	7.2–54.2	6.0–52.8
Collected refl.	28956	26506	50197	50387	55165
Independent refl.	5006	6830	11067	11811	11281
Obs. refl. [<i>F</i> ₀ ≥ 4 σ (<i>F</i>)]	4220	5283	8952	8392	9707
No. ref. param.	282	350	619	691	691
<i>R</i> ₁ [<i>F</i> ₀ ≥ 4 σ (<i>F</i>)]	0.0418	0.00433	0.0382	0.0382	0.0445
<i>wR</i> ₂ (all data)	0.0930	0.0897	0.0782	0.0819	0.1088
Goof (<i>F</i> ²)	1.024	1.036	0.919	0.834	1.044
Absolute structure parameter <i>x</i>	−0.05(7)	−0.05(3)	−0.02(2)	0.01(3)	−0.01(3)
Max.; min. res. electron density, e Å ⁻³	0.47; −0.34	0.62; −0.75	0.46; −0.41	0.96; −0.52	1.02; −0.85

omers generated by these two centers and the preservation of the absolute configuration of the particular ligand backbones would be a good explanation for this experimental finding, and this agrees with the NMR results (*vide infra*). A slight bathochromic shift of the absorption of the complex cations accounts for the complexation of the chelate ligands. Only for **16** a positive medium Cotton effect is observed in the 380–410 nm region of the Ru(II) transitions [4e, 10], whereas for the η^6 -mesitylene complexes **17**–**19** the Cotton effects in that region are much weaker, but also positive. This points to the dominance of one enantiomer with the chiral Ru(II) center of **16** in the sample. As the benzylic ligand backbone C* stereocenter is stable and identical with that in the ligand used, it is left to the chiral sulfur center of **16** to be affected by an epimerization equilibrium in solution. Complementarily, the corresponding weak Cotton effects for **17**–**19** indicate an epimerization equilibrium at both, the chiral Ru(II) and the sulfur center due to the pseudo-enantiomeric relationship of

their *as* and *sa* as well as of their *aa* and *ss* diastereomers.

The NMR spectrum of the η^6 -(*p*-cymene) cation **16** consists of two sets of signals belonging to two diastereomers. Their intensity ratio of 1 : 0.32 is independent of the work-up procedure applied, a good hint to a chemical equilibrium in solution as the reason. The ratio is only slightly influenced by temperature (Fig. 7) and by solvent (Table 11), however, significant line broadening is observed at ambient and higher temperature which is absent at −30 °C. No coalescence of signals could be observed up to +70 °C. As for the mesitylene species **17**–**19** (*vide infra*), the effect is related to an increasing exchange rate between the diastereomers of **16**. At −30 °C the aromatic η^6 -(*p*-cymene) protons split completely into two sets of four doublets for each diastereomer due to their planar diastereotopicity (Fig. 7). At the same time no significant signal changes are observable for the chelate ring phenyl substituents, thus free rotation around their C*–C and S*–C bonds,

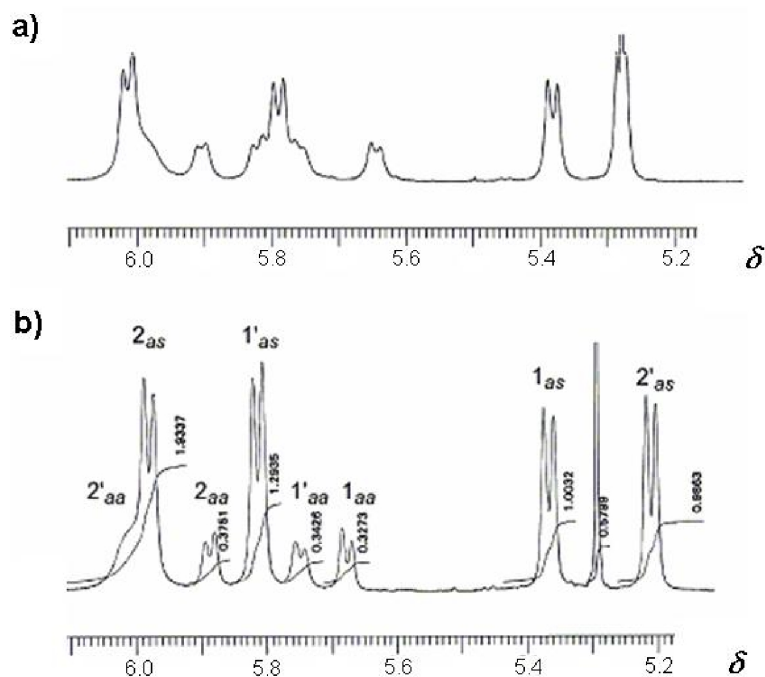
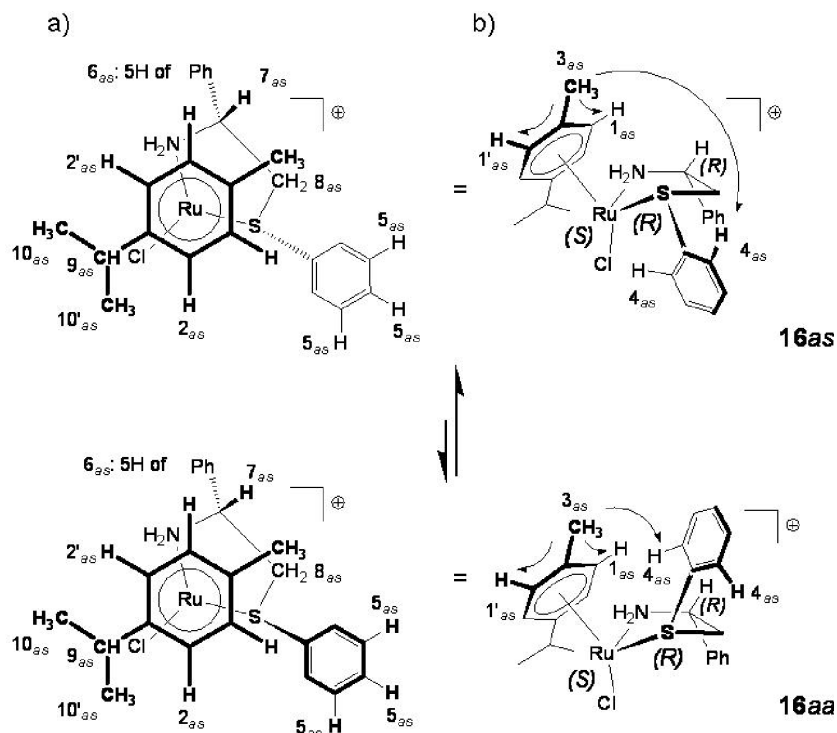


Fig. 7. Aromatic η^6 -(*p*-cymene) proton region of the ^1H NMR spectra of **16** (CDCl_3 , 400 MHz); a) ambient temperature; b) $-30\text{ }^\circ\text{C}$; for numbering see Scheme 4.



Scheme 4. Diastereomers of **16as** and **16aa** in equilibrium; a) Numbering of protons not affected upon NOE irradiation; b) NOE responses and numbering of protons affected by irradiation of the *p*-methyl group of the η^6 -(*p*-cymene) ligand.

respectively, is assumed for both of them. NOE irradiations at the two *p*-methyl singlets of the η^6 -(*p*-cymene) ligand (Scheme 4, Fig. 8) lead to the response

of the two sets of the corresponding (2,6)-protons of the arene ligand and of the *ortho* protons of the thiophenyl ring only. No NOE response could be observed

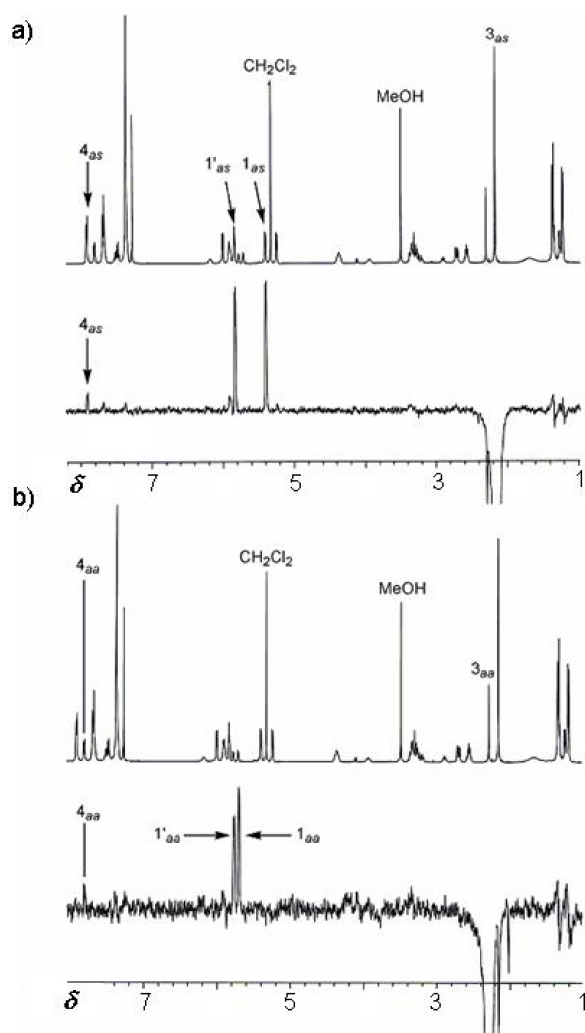


Fig. 8. NOE irradiation on the *p*-methyl groups of the η^6 -(*p*-cymene) ligands of a) **16_{as}** and b) **16_{aa}**; for numbering see Scheme 4.

for the protons of the ligand backbone phenyl substituents (7.34 ppm, *m*).

Evidence is obtained from the CD spectrum of **16** that both diastereomers must have the same absolute configuration at the Ru(II) center, leaving the choice only to the *as* + *aa* or the *sa* + *ss* pairs of diastereomers. Therefore the absence of a NOE response of the ligand backbone phenyl substituents suggests that these phenyl rings are in *anti* position to the η^6 -(*p*-cymene) ligand. This leaves finally the choice to the *as* + *aa* pair of diastereomers only. The A^{1,2} repulsion of the thiophenyl moiety from the coordinated arene must be expected to be weaker for the *as* than for the

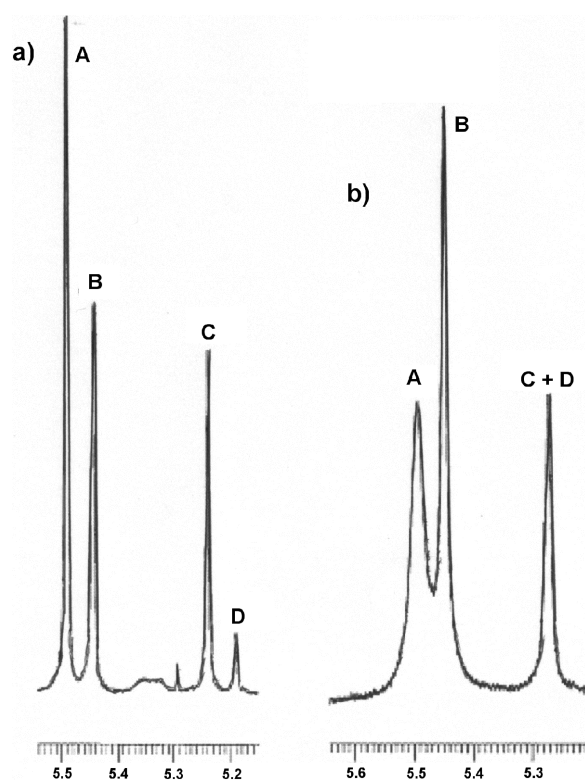


Fig. 9. Aromatic η^6 -mesitylene proton region ($\delta = 5\text{--}6$) of the ^1H NMR spectra of **17** (CDCl_3 , 400 MHz); a) at $-30\text{ }^\circ\text{C}$; b) at ambient temperature.

aa diastereomer, so that the *as* should be energetically preferred over the *aa* diastereomer. Thus, the signals belonging to the major species present in solution are assigned to the *as* diastereomer of **16**. All other ^1H resonances were assigned by $J(\text{H})/(\text{H})\text{-COSY}$, by coupling constants and/or similarity relationships, which were then correlated to the signals in the ^{13}C NMR spectrum by DEPT and HMQC experiments.

A completely different situation is observed for the η^6 -mesitylene species **17–19** in solution (Fig. 9). The aromatic protons of the π -mesitylene ligand (5.2–5.8 ppm) form singlets of different intensity for each diastereomer distinguishable by NMR due to its C_3 symmetry. A hindered rotation of the π -arene ligands can be ruled out as the reason for that finding, as no intensity ratios or temperature dependence effects were observed, which would fit to such a model. As a consequence, free rotation of the π -mesitylene ligands even at low temperature has to be assumed. The same manifold of proton NMR singlets appears for the mesitylene methyl protons (1.5–2.4 ppm), and integration of both

sets of signals can be principally used for the determination of the diastereomer ratios. Three broadened singlets are generally observable at ambient temperature and four sharper ones at low temperature. If the four lines are related to the NMR-distinguishable diastereomers of **17–19**, the observation fits to structures with two configurationally labile stereocenters, both in equilibrium with their optical antipodes. The broadened and partially collapsed ambient temperature spectra suggest increasing exchange rates between diastereomers, however, no rapid exchange limit spectra could be reached at elevated temperatures. As **17–19** exhibit three stereocenters each, one of them is excluded from forming the observed diastereomers. As for the CD spectra, we assign this to the designed chiral benzylic carbon atom of the chelate ring backbone, which was identified exclusively in its *R* configuration in the solid state.

An example is given for **17** in CDCl₃ (Fig. 9). Four singlets **A–D** with an intensity ratio of 1 : 0.6 : 0.5 : 0.05 appear at –30 °C. They are all broadened, and **C + D** collapse into one line at r. t., yielding an intensity ratio of 1.0 : 0.36 : 0.29. An increase of temperature by 50 °C thus caused only a small change of the relative diastereomer ratios of **17**.

As a consequence, the four identified arene proton signals **A–D** of the mesitylene ligand of **17** can be related to the four possible diastereomers **17as**, **sa**, **aa**, and **ss**. The most intense signal **A** which is located at the low-field side of the π -arene NMR region can be assigned to the energetically most favored species **17as** with its minimal axial repulsion effects between the two substituents of the five-membered chelate ring and the mesitylene ligand, and the smallest signal **D** must belong to the most disfavored diastereomer **17ss**. On the other hand, no clear relations between signals **B** and **C** and **17sa** and **17aa**, respectively, can be elucidated due to their small differences, both in intensity and chemical shift. The effect was studied in different solvents with no principal differences between them.

In conclusion, from the NMR spectroscopic results evidence has been found for low inversion barriers for both, the chiral sulfur center as well as the ruthenium atom in its chiral [Ru(η^6 -arene)(N \cap S)Cl] coordination sphere, and for a free rotation of the η^6 -bonded arene ligands.

Conclusions

Five enantiopure β -aminothioethers were obtained by different routes orientated on literature protocols.

Three of them were reacted successfully with two di- μ -chloro-bis{chloro[η^6 -arene]ruthenium(II)} derivatives, resulting in the title complex salts. The complex cations exhibit three stereocenters, the ruthenium and sulfur atoms and the chiral benzylic carbon atom of the chelate ligand backbone. The η^6 -*p*-cymene species **16** forms two diastereomers only with an epimerized sulfur atom, but a defined ruthenium stereocenter. The chiral benzylic carbon atoms of the chelate ligands are completely stable for all species investigated under all conditions applied so far. The relative diastereomer concentrations in solution depend mainly on the spatial requirements of the η^6 -arene ligand rather than on the chiral carbon atom or thioether substituents of the chelate ligand. The η^6 -*p*-cymene ligand of **16** is inducing a dominating A^{1,2}-repulsion of the N \cap S chelate ligand S*-phenyl moiety and forces it exclusively into the *anti* positions of **16as** and **16aa** diastereomers with their common (*S*)-configuration of the chiral Ru(II) centers. In agreement with the spectroscopic results, only the energetically most preferred diastereomer **16as** has been observed in the crystalline state allowing the determination of its absolute configuration.

Both, the ruthenium and sulfur stereocenters of the complexes epimerize in solution into a mixture of four NMR distinguishable *as*, *sa*, *aa*, and *ss* diastereomers in an equilibrium for the smaller η^6 -mesitylene ligands of cations **17–19**. Again, the spectroscopic findings are confirmed by the results of X-ray structure studies. All single crystals of the PF₆ salts of cations **17–19** investigated contain *as* and *sa* diastereomers in the ratio 1 : 1 and allowed the determination of their absolute structure parameters in the solid state.

With respect to the long term targets of these investigations, compounds **16** and **17** were tested as catalysts in the transfer hydrogenation of acetophenone with isopropanol under basic conditions [3b–j]. They are active but not enantioselective.

Experimental Section

General

All reactions were carried out under N₂ by using conventional Schlenk techniques. Liquid reagents were generally added with disposable plastic syringes. All work-ups were performed in air. Complex cations **16–19** are airstable in the solid state and only slightly airsensitive in solution. Except **11**, all other substances prepared are also airstable. Solvents and chemicals were purchased from Acros, Aldrich, Strem, and Merck. Solvents, Et₃N and mesyl chloride were dried and distilled under N₂

prior to use: THF over sodium/benzophenone; MeOH and *n*-PrOH over magnesium, CH₂Cl₂ and Et₃N over calcium hydride. All other solvents and chemicals were used as received. (–)-(R)-2-Amino-2-phenylethanol **1** [6a], (–)-(2R)-2-[(1',1'-dimethylethoxy-carbonyl)amino]-2-phenylethanol **2** [6b], (4R)-4-phenyl-2-oxalodinone **8** [7a, b], di- μ -chloro-bis[chloro{ η^6 -[1-methyl-4-(methylethyl)benzene]}ruthenium(II)] **14** [8a, b] and di- μ -chlorobis{chloro[η^6 -(1,3,5-trimethylbenzene)]ruthenium(II)} **15** [8a] were prepared as reported. Flash column chromatography (FC): silica gel F 60 (Fluka or Merck). Thin layer chromatography (TLC): Merck F 60 silica plates with a 364 nm fluorescence indicator; primary amines were identified by spraying with a ninhydrine soln. and heating of the TLC plates. Melting points: Büchi 530 melting point apparatus; not corrected. Polarimetric measurements: Perkin-Elmer 341 polarimeter. Circular dichroism measurements: JASCO J-710 spectropolarimeter. NMR spectra: Jeol FT-JNM-EX 270 (270 MHz), Bruker AMX 300 (300 MHz), Jeol FT-JNM-LA 400 (400 MHz) and Jeol A 500 (500 MHz) spectrometers; in deuterated solvents and referenced to the residual proton signal of the particular solvent. ¹H and ¹³C NMR signals were generally assigned by utilizing ¹J(H)¹J(H)-COSY, DEPT and HMQC techniques. Mass spectra: Varian MAT 212 spectrometer. Elemental analyses: Carlo Erba elemental analyzer Model 1108.

(–)-(1R)-1-[(1',1'-Dimethylethoxycarbonyl)amino]-2-(methylsulfonyl)oxy-1-phenylethane (**3**)

To **2** (24.86 g, 105 mmol) and Et₃N (22.0 mL, 158 mmol) in CH₂Cl₂ (300 mL) at 0 °C, within 10 min mesyl chloride (10.0 mL, 129 mmol) was added dropwise. The mixture was stirred for 16 h in the cooling bath for defrosting to r.t. The soln. was poured into a sat. NaHCO₃ soln., and the organic phase washed once with brine, dried (MgSO₄), and concentrated to afford 29.53 g (89 %) of **3** as a slightly yellowish powder. For prolonged times, the solid product should be stored at 0 °C. M.p. 82 °C starting dec. – [α]_D²³ = –29.2 (CH₂Cl₂, *c* = 0.0082). – ¹H NMR ([D₆]DMSO, 270 MHz): δ = 7.71 (br pseudo d, 1H, -NH(BOC)), 7.36–7.26 (m, 5H, Ph), 4.85 (not res. dd, 1H, -CH-), 4.23 (2 not res. dd, 2H, -CH₂-), 3.14 (s, 3H, -SO₂CH₃), 1.34 (br s, 9H, -C(CH₃)₃). – ¹³C{¹H} NMR ([D₆]DMSO, 68 MHz, dominant rotamer): δ = 154.85 (-CO-), 138.78 (*C*_{ipso} of Ph), 128.30 (*C*_m of Ph), 127.53 (*C*_p of Ph), 126.93 (*C*_o of Ph), 78.22 (-C(CH₃)₃), 71.30 (-CH₂-), 53.30 (-CH-), 36.86 (-SO₂CH₃), 28.21 (-C(CH₃)₃). – FD-MS (pos.; CH₂Cl₂): *m/z* (%) = 163 (100) [C₉H₉NO₂]⁺, 316 (71) [M]⁺. A correct elemental analysis could not be obtained.

(–)-(1R)-1-Phenyl-2-[(phenylmethyl)thio]ethylamine (**4**)

a) Representative procedure: To benzylthiol (4.00 mL, 34.07 mmol) in THF (100 mL) and MeOH (30 mL) at

r.t. were added *t*-BuOK (3.801 g, 33.87 mmol) and then **3** (5.100 g, 16.17 mmol). Potassium mesylate started to precipitate immediately. After stirring for 12 h at r.t., 30 mL 36 % HCl was added, and the mixture was stirred for another 30 min before concentration *in vacuo* (max. 60 °C/10 mbar). The residue was suspended in 40 % NaOH and the aqueous phase extracted twice with CH₂Cl₂. The combined organic layers were dried (Na₂SO₄) and concentrated to get 3.926 g (> 99 %) of **4** as a slightly yellowish oil which contains traces of **8**.

b) Representative procedure: After dissolving Na (661 mg, 28.75 mmol) in *n*-PrOH (30 mL), benzylthiol (5.20 mL, 44.29 mmol) and solid **8** (2.062 g, 12.64 mmol) were added at r.t. The soln. was heated for 24 h under reflux. After cooling to r.t., the soln. was poured into a threefold volume of 40 % NaOH and extracted once with CH₂Cl₂. The organic phase was washed twice with 40 % NaOH to remove excess thiol, dried (Na₂SO₄) and concentrated: 2.706 g (88 %) of crude product as turbid yellow oil, which was purified by Kugelrohr distillation: 2.586 g (84 %; b.p. > 160 °C/0.0001 mbar) of **4** as clear and colorless oil. – [α]_D²³ = –46.2 (CH₂Cl₂, *c* = 0.0017). – ¹H NMR (CDCl₃, 270 MHz): δ = 7.34–7.19 (2 m, 10H, Ph), 3.99 (dd, ³*J* = 8.9, ³*J* = 4.3 Hz, 1H, -CH-), 3.65 (s, 2H, -S-CH₂-Ph), 2.73 (dd, ²*J* = 13.5, ³*J* = 4.3 Hz, 1H, -CH(NH₂)-CH₂-), 3.53 (dd, ²*J* = 13.5, ³*J* = 8.9 Hz, 1H, -CH(NH₂)-CH₂-), 1.77 (br s, 2H, -NH₂). – ¹³C{¹H} NMR (CDCl₃, 68 MHz): δ = 144.26 (*C*_{ipso} of Ph-CH-), 138.04 (*C*_{ipso} of -S-CH₂-Ph), 128.69 (*C*_m of Ph-CH-), 128.30 (*C*_o of -S-CH₂-Ph), 128.29 (*C*_m of -S-CH₂-Ph), 127.16 (*C*_m of Ph-CH-), 126.85 (*C*_p of -S-CH₂-Ph), 126.14 (*C*_o of Ph-CH-), 54.60 (-CH-), 41.16 (-CH(NH₂)-CH₂-), 36.40 (-S-CH₂-Ph). – FD-MS (pos.; CH₂Cl₂): *m/z* (%) = 244 (100) [M + H]⁺. A correct elemental analysis could not be obtained.

(+)-(1R)-1-Phenyl-2-(phenylthio)ethylamine (**5**)

a) According to the above procedure from thiophenol (2.00 mL, 21.31 mmol), *t*-BuOK (2.353 g, 20.97 mmol) and **3** (3.047 g, 9.66 mmol) in MeOH (20 mL) for 18 h. Reaction monitored with FD-MS (reaction mixture diluted with CH₂Cl₂): *m/z* (%) = 329 (100) [Ph-CH[NH(BOC)]-CH₂-SPh]⁺: 2.289 g of crude **5** as a yellow oil, which contained *ca.* 20 % **8** (NMR). The crude product was recrystallized twice from hot EtOH layered with pentanes by slowly cooling down to –30 °C; this and recrystallization of the combined mother liquors afforded overall 1.559 g (70 %) of **5** as white crystals.

b) The original procedure was modified [7c, d]. According to the above procedure from Na (290 mg, 12.61 mmol), thiophenol (2.00 mL, 21.31 mmol) and **8** (604 mg, 3.70 mmol) in *n*-PrOH (20 mL) for 12 h under reflux: 790 g (93 %) crude product as brownish microcrystals, recrystallized from EtOH and some drops of hexanes at –30 °C: 636 mg (75 %) of **5**. –

M. p. = 72–73 °C (lit: 69–70 °C). – $[\alpha]_D^{23} = +29.4$ (CH₂Cl₂, $c = 0.0042$); $[\alpha]_D^{23}$ (lit. for (*S*)-enantiomer) = –24.2 (CHCl₃, $c = 1.00$). NMR and MS spectra of **5** in full agreement with those reported [7c, d].

(–)-(1*R*)-1-Phenyl-2-(1'-naphthylthio)ethylamine (**6**)

According to the above procedure from α -thionaphthol (3.03 mL, 21.74 mmol), *t*-BuOK (2.445 g, 21.79 mmol) and (6.833 g, 21.67 mmol) **3** in MeOH (20 mL) for 20 h: 5.632 g (93 %) of crude **6** as a brown turbid oil containing traces of **8** (NMR), which was purified twice by FC [gradient elution with hexanes/CH₂Cl₂/MeOH 1 : 1 : 0 (→ impurities) and then with 10 : 10 : 1 (→ **6**): 3.191 g (53 %; $R_f = 0.01$ [TLC, hexanes/CH₂Cl₂ 1 : 1], $R_f = 0.28$ [TLC, hexanes/CH₂Cl₂/MeOH 10 : 10 : 1]) **6** as yellowish oil with traces of impurities (NMR). – $[\alpha]_D^{23} = -5.5$ (CH₂Cl₂, $c = 0.0195$), $[\alpha]_D^{23} = -11.8$ (CHCl₃, $c = 0.1992$). – ¹H NMR (CDCl₃, 270 MHz): $\delta = 8.37$ (pseudo d, 1H, H-C(5 or 8) of α -Naph), 7.81–7.16 (series of m, 11H, Ph, α -Naph), 4.01 (dd, ³*J* = 9.4, ³*J* = 4.0 Hz, 1H, -CH-), 3.27 (dd, ²*J* = 13.1, ³*J* = 4.0 Hz, 1H, -CH₂-), 3.03 (dd, ²*J* = 13.1, ³*J* = 9.4 Hz, 1H, -CH₂-), 1.78 (br s, 2H, -NH₂). – ¹³C{¹H} NMR $\delta =$ (CDCl₃, 68 MHz): 143.86 (*C*_{ipso} of Ph), 133.62 (C(1) of α -Naph), 132.69 (C(4a) of α -Naph), 132.66 (C(8a) of α -Naph), 128.35 (C(5) of α -Naph), 128.30 (C(8) of α -Naph), 128.16 (*C*_m of Ph), 127.21 (*C*_p of Ph), 127.09 (C(3) of α -Naph), 126.18 (C(6) of α -Naph), 126.05 (*C*_o of Ph), 125.94 (C(7) of α -Naph), 125.22 (C(4) of α -Naph), 124.73 (C(2) of α -Naph), 54.33 (-CH-), 43.85 (-CH₂-). – FD-MS (pos.; CH₂Cl₂): m/z (%) = 280 (100) [M + H]⁺. A correct elemental analysis could not be obtained.

(+)-(1*R*)-1-Phenyl-2-(2'-naphthylthio)ethylamine (**7**)

a) According to the above procedure from β -thionaphthol (1.690 g, 10.55 mmol), *t*-BuOK (1.183 g, 10.54 mmol) and **3** (2.997 g, 9.50 mmol) in MeOH (20 mL) for 19 h. Reaction monitored with FD-MS (reaction mixture diluted with CH₂Cl₂): m/z (%) = 379 (100) [Ph-CH[NH(BOC)]-CH₂-S(β -Naph)⁺]: 2.344 g of crude **7** as a brown oil, containing ca. 20 % **8** (NMR). The crude product was recrystallized three times from a minimum amount of hot CHCl₃ layered with the double amount of pentane, cooled slowly from r. t. down to –30 °C: 757 mg (29 %) of **7** with traces of **8**.

b) According to the above procedure from Na (642 mg, 27.93 mmol), β -thionaphthol (7.519 g, 56.92 mmol) and **8** (1.064 g, 6.52 mmol) in ⁿPrOH (40 mL) for 18 h under reflux. 3.652 g of crude **7** was isolated as a yellowish solid. The crude product was purified twice by FC (hexanes/CH₂Cl₂/MeOH = 10 : 10 : 1) and then recrystallized twice as described above: 475 mg [26 %; $R_f = 0.38$ (TLC)] of **7** as brownish microcrystals. – M. p. = 98–99 °C. – $[\alpha]_D^{23} = +63.7$ (CH₂Cl₂, $c = 0.0029$). – ¹H NMR

(CDCl₃, 270 MHz): $\delta = 7.74$ –7.66 (m, 4H, H-C(5,6,7,8) of β -Naph), 7.45–7.14 (series of m, 8H, Ph, β -Naph), 4.07 (dd, ³*J* = 9.3, ³*J* = 4.0 Hz, 1H, -CH-), 3.34 (dd, ²*J* = 13.4, ³*J* = 4.0 Hz, 1H, -CH₂-), 3.05 (dd, ²*J* = 13.4, ³*J* = 9.3 Hz, 1H, -CH₂-), 1.64 (br s, 2H, -NH₂). – ¹³C{¹H} NMR (CDCl₃, 68 MHz): $\delta = 144.21$ (*C*_{ipso} of Ph), 133.65 (C(8a) of β -Naph), 133.11 (C(2) of β -Naph), 131.81 (C(4a) of β -Naph), 128.57 (*C*_m of Ph), 128.50 (C(4) of β -Naph), 127.64 (*C*_p of Ph), 127.56 (C(8) of β -Naph), 127.55 (C(5) of β -Naph), 127.03 (C(6,7) of β -Naph), 126.55 (C(1) of β -Naph), 126.34 (*C*_o of Ph), 125.76 (C(3) of β -Naph), 54.70 (-CH-), 43.71 (-CH₂-). – FD-MS (pos.; CH₂Cl₂): m/z (%) = 280 (100) [M + H]⁺. A correct elemental analysis could not be obtained.

(–)-(1*R*)-1-Phenyl-2-(1'-naphthylthio)ethylammonium 4-methylphenyl-sulfonate (**9**)

From a saturated solution of crude **6** (3.409 g, ca. 12.20 mmol) and *p*-tosic acid monohydrate (2.339 g, 12.30 mmol) in EtOH at –30 °C as white needles. 1.715 g (31 %) of crystalline **9** was isolated after recrystallization (X-ray crystal structure analysis). – M. p. = 169–170 °C. – $[\alpha]_D^{23} = +14.0$ (MeOH, $c = 0.0053$). – ¹H NMR ([D₆]DMSO, 300 MHz): $\delta = 8.50$ (br s, 3H, -NH₃⁺), 8.25–7.27 (series of m, 12H, Ph, α -Naph), 7.89 (d, ²*J* = 8.3 Hz, 2H, H-C(3,5) of *p*-TolSO₃[–]), 7.08 (d, ²*J* = 8.3 Hz, 2H, H-C(2,6) of *p*-TolSO₃[–]), 4.39 (dd, ³*J* = 8.6, ³*J* = 6.0 Hz, 1H, -CH-), 3.61 (dd, ²*J* = 13.6, ³*J* = 6.0 Hz, 1H, -CH₂-), 3.51 (dd, ²*J* = 13.6, ³*J* = 8.6 Hz, 1H, -CH₂-), 2.29 (s, 3H, -CH₃ of *p*-TolSO₃[–]). – ¹³C{¹H} NMR ([D₆]DMSO, 75 MHz): $\delta = 145.48$ (*C*_{ipso} of Ph), 137.74 (C(1) of *p*-TolSO₃[–]), 136.12 (C(4) of *p*-TolSO₃[–]), 133.76–124.26 (Ph, α -Naph, *p*-TolSO₃[–]), 53.51 (-CH-), 37.04 (-CH₂-), 20.76 (-CH₃ of *p*-TolSO₃[–]). A correct elemental analysis could not be obtained.

(–)-(2*R*)-2-Amino-2-phenylethanethiol hydrochloride (**10**)

To a deep blue soln. of Na (1.861 g, 80.95 mmol) in liquid NH₃ (165 mL) at –80 °C were calcuated within 2 min from a Schlenk flask **4** (4.036 g, 16.58 mmol) and *t*-BuOH (1.548 g, 20.89 mmol) dissolved in THF (40 mL). The blue soln. was stirred for 45 min first inside the cooling bath, then for 1 h outside until the reaction was quenched with excess of ammonium chloride. NH₃ was evaporated with nitrogen gas, the residue suspended in EtOH, acidified to pH = 1–2 with 36 % HCl and the soln. filtered off from NaCl. The clear soln. was evaporated to dryness, the white residue dissolved in CH₂Cl₂/*i*PrOH/MeCN 1 : 1 : 1 and filtered off from residual NaCl again. After solvent evaporation the crude product was dissolved in CH₂Cl₂, precipitated with Et₂O, filtered off and dried (P₂O₅, vacuum): 2.389 g (76 %) of **10** as an almost colorless powder. – M. p. = 153–155 °C. – $[\alpha]_D^{23} = -7.5$ (MeOH, $c = 0.00296$). – ¹H NMR ([D₆]DMSO, 270 MHz):

$\delta = 8.77$ (br s, 3H, $-\text{NH}_3^+$), 7.53–7.10 (m, 5H, Ph), 4.32 (not res. dd, 1H, $-\text{CH}-$), 3.34 (s, 1H, $-\text{SH}$), 3.08–2.85 (2 not res. dd, 2H, $-\text{CH}_2-$). – $^{13}\text{C}\{^1\text{H}\}$ NMR ($[\text{D}_6]\text{DMSO}$, 68 MHz): $\delta = 136.33$ (C_{ipso} of Ph), 128.62 (C_p of Ph), 128.51 (C_m of Ph), 127.58 (C_o of Ph), 56.35 ($-\text{CH}-$), 27.91 ($-\text{CH}_2-$). A correct elemental analysis could not be obtained.

NMR characterization as (-)-(2R)-2-amino-2-phenylethanthiol (II)

An analytical aliquot of **10** mixed with Na_2CO_3 in MeOH (*ca.* 3 mL) and *aqua dest.* (0.1 mL) was evaporated to dryness, the residue dissolved in CDCl_3 , filtered and dried. – ^1H NMR (CDCl_3 , 270 MHz): $\delta = 7.40$ –7.15 (m, 5H, Ph), 4.26 (dd, $^3J = 9.2$, $^3J = 4.0$ Hz, 1H, $-\text{CH}-$), 3.01 (dd, $^2J = 13.4$, $^3J = 4.0$ Hz, 1H, $-\text{CH}_2-$), 2.78 (dd, $^2J = 13.4$, $^3J = 9.2$ Hz, 1H, $-\text{CH}_2-$), 1.76 (2 br s, 3H, $-\text{SH}$, $-\text{NH}_2$). – $^{13}\text{C}\{^1\text{H}\}$ NMR (CDCl_3 , 68 MHz): $\delta = 143.87$ (C_{ipso} of Ph), 128.55 (C_m of Ph), 127.45 (C_p of Ph), 126.42 (C_o of Ph), 54.34 ($-\text{CH}-$), 43.58 ($-\text{CH}_2-$).

(-)-(2R)-[(1',1'-Dimethylethoxycarbonyl)amino]-2-phenylethanthiol (12)

To KSAc (3.815 g, 33.40 mmol) in MeOH (50 mL) and THF (50 mL) was added **3** (7.063 g, 22.39 mmol), the suspension stirred for 24 h at r.t., then saturated for 10 min with $\text{NH}_3(\text{gas})$ and stirred overnight. After concentration, the residue was suspended in EtOAc, washed once with 1 % HCl and then three times with brine. The organic phase was dried (MgSO_4), concentrated to afford 4.146 g crude product containing considerable amounts of **8** (NMR), and purified by FC [applied as solid; gradient elution with hexanes/EtOAc 2 : 1 (\rightarrow **12**), then with CH_2Cl_2 (\rightarrow **8**): 2.212 g [40 %; $R_f = 0.41$ (TLC, hexanes/EtOAc 2 : 1)] of **12** as a yellowish powder and 225 mg [6 %; $R_f = 0.07$ (TLC, hexanes/EtOAc 2 : 1)] of **8**. – M. p. = 144 °C. – $[\alpha]_{\text{D}}^{23} = -47.3$ (CH_2Cl_2 , $c = 0.0030$). – ^1H NMR ($[\text{D}_6]\text{DMSO}$, 270 MHz): $\delta = 7.29$ –7.18 (m, 5H, Ph), 4.75–4.46 (partly res. dd, 1H, $-\text{CH}-$), 3.14–2.97 (partly res. dd, 2H, $-\text{CH}_2-$), 2.28 (s, 1H, $-\text{SH}$), 1.29–1.11 (2 br s of rotamers, 9H, $-\text{C}(\text{CH}_3)_3$). – $^{13}\text{C}\{^1\text{H}\}$ NMR ($[\text{D}_6]\text{DMSO}$, 75 MHz, at least 3 rotamers): $\delta = 154.94$ ($-\text{CO}-$), 142.34 (C_{ipso} of Ph), 128.33 (C_m of Ph), 127.19 (C_p of Ph), 126.27 (C_o of Ph), 77.98 ($-\text{C}(\text{CH}_3)_3$), 66.98 ($-\text{CH}-$), 54.08 ($-\text{CH}-$), 34.85 ($-\text{CH}_2-$), 30.47 ($-\text{C}(\text{CH}_3)_3$), 28.15 ($-\text{C}(\text{CH}_3)_3$), 25.07 ($-\text{C}(\text{CH}_3)_3$). – FD-MS (pos.; CH_2Cl_2): m/z (%) = 504 (100) $[2\text{M} - 2\text{H}]^+$. A correct elemental analysis could not be obtained.

(-)-(1R)-1-Phenyl-2-[(3'-methylbut-2'-enyl)thio]ethylamine (13)

a) To **10** (1.180 g, 6.22 mmol) and *t*-BuOK (1.264 g, 11.26 mmol) in MeOH (35 mL) was added prenyl bromide

(0.82 mL, 6.99 mmol). After stirring for 19 h at r.t. 2 mL 36 % HCl was added, the soln. stirred for 10 min and concentrated *in vacuo* (max. 60 °C/10 mbar). The slurry was suspended in *aqua dest.*, brought to pH = 14 with 40 % NaOH, and the aqueous phase extracted twice with Et_2O . The combined organic layers were dried (Na_2SO_4) and concentrated: 1.369 g (99 %) nearly pure **13** as an orange oil. Spectroscopic data see below.

b) To **12** (1.201 g, 4.74 mmol) and *t*-BuOK (585 g, 5.21 mmol) in THF (35 mL) was added prenyl bromide (0.66 mL, 5.62 mmol). After stirring for 19 h at r.t. 10 mL 36 % HCl was added, the soln. stirred for 40 min (open flask) before work-up as described above: 1.006 g (96 %) nearly pure **13** as slight brownish oil. Purification: FC (hexanes/ CH_2Cl_2 /MeOH 10 : 10 : 1): 831 mg [34 % average; $R_f = 0.37$ (TLC)] **13** as yellowish oil. – $[\alpha]_{\text{D}}^{23} = -38.1$ (CHCl_3 , $c = 0.114$). – ^1H NMR (CDCl_3 , 270 MHz): $\delta = 7.33$ –7.24 (m, 5H, Ph), 5.20 (pseudo t, 1H, $-\text{CH}=\text{C}(\text{CH}_3)_2$), 4.05 (dd, $^3J = 9.2$, $^3J = 4.04$ Hz, 1H, $-\text{CH}-$), 3.11 (m, 2H, $-\text{CH}_2-\text{CH}=\text{C}(\text{CH}_3)_2$), 2.78 (dd, $^2J = 13.4$, $^3J = 4.0$ Hz, 1H, $-\text{CH}(\text{NH}_2)-\text{CH}_2-$), 2.59 (dd, $^2J = 13.4$, $^3J = 9.2$ Hz, 1H, $-\text{CH}(\text{NH}_2)-\text{CH}_2-$), 1.76 (s, 2H, $-\text{NH}_2$), 1.71 (not res. d, 3H, $-\text{CH}=\text{C}(\text{CH}_3)_{\text{cis}}(\text{CH}_3)$), 1.64 (partly res. d, 3H, $-\text{CH}=\text{C}(\text{CH}_3)_{\text{trans}}(\text{CH}_3)$). – $^{13}\text{C}\{^1\text{H}\}$ NMR (CDCl_3 , 68 MHz): $\delta = 144.47$ (C_{ipso} of Ph), 135.04 ($-\text{CH}=\text{C}(\text{CH}_3)_2$), 128.25 (C_m of Ph), 127.08 (C_p of Ph), 126.11 (C_o of Ph), 120.39 ($-\text{CH}_2-\text{CH}=\text{C}(\text{CH}_3)_2$), 54.82 ($-\text{CH}(\text{NH}_2)-\text{CH}_2-$), 41.10 ($-\text{CH}(\text{NH}_2)-\text{CH}_2-$), 29.63 ($-\text{CH}_2-\text{CH}=\text{C}(\text{CH}_3)_2$), 25.60 ($-\text{CH}=\text{C}(\text{CH}_3)_{\text{cis}}(\text{CH}_3)$), 17.74 ($-\text{CH}=\text{C}(\text{CH}_3)_{\text{trans}}(\text{CH}_3)$). – FD-MS (pos.; CH_2Cl_2): m/z (%) = 222 (100) $[\text{M} + \text{H}]^+$. A correct elemental analysis could not be obtained.

[(+)-(R_{Ru}, 1'' R)-Chloro- η^6 -[1-methyl-4-(1'-methylethyl)-benzene]- σ (N): σ (S)-[1''-phenyl-2''-(phenylthio)ethyl-amino]ruthenium(II)] hexafluorophosphate, [16][PF₆]

Representative procedure: In MeOH (25 mL) **14** (606 mg, 0.990 mmol) and **5** (471 mg, 2.054 mmol) were stirred at r.t. until they were completely dissolved (40 min; \rightarrow clear yellow soln.). After addition of NaPF_6 (587 mg, 3.495 mmol), the mixture was stirred for 17 h at r.t., concentrated, the residue dissolved in CH_2Cl_2 and filtered. After concentration the product was crystallized from a saturated solution ($\text{MeOH}/\text{CH}_2\text{Cl}_2$ 1 : 1) overnight at -30 °C to yield 956 mg (67 %) of **[16][PF₆]** as yellow needles. The crystalline material contains one molecule of MeOH and half a molecule of CH_2Cl_2 per formula unit (analytical data, X-ray crystal structure analysis). – M. p. = 105–106 °C. – $[\alpha]_{\text{D}}^{23} = +10.3$ (CH_2Cl_2 , $c = 0.00276$). – ^1H NMR (CDCl_3 , 400 MHz, -30 °C; contains CH_2Cl_2 and MeOH; integration referenced to methyl singlet of the η^6 -(*p*-cymene) ligand assigned to the *as* diastereomer): $\delta = 7.90$ –7.88 (pseudo d, 2H, H_o of

Ph-S-, *as*), 7.78–7.76 (pseudo d, 0.64H, H_o of Ph-S-, *aa*), 7.67–7.61 (m, 3H, $H_{m,p}$ of Ph-S-, *as*), 7.50–7.42 (m, 0.96H, $H_{m,p}$ of Ph-S-, *aa*), 7.34 (m, 7.92H, *Ph-CH-*, *as* and *aa*), 6.28 (br s, 2.64H, -NH₂-, *as* and *aa*), 6.06–6.0 (not res. d, 0.32H, H–C(3 or 5) of η^6 -(*p*-cymene), *aa*), 5.98 (d, $^3J = 5.8$ Hz, 1H, H–C(3 or 5) of η^6 -(*p*-cymene), *as*), 5.89 (d, $^3J = 5.8$ Hz, 0.32H, H–C(5 or 3) of η^6 -(*p*-cymene), *aa*), 5.81 (d, $^3J = 5.8$ Hz, 1H, H–C(6 or 2) of η^6 -(*p*-cymene), *as*), 5.75 (d, $^3J = 5.83$ Hz, 0.32H, H–C(2 or 6) of η^6 -(*p*-cymene), *aa*), 5.68 (d, $^3J = 5.8$ Hz, 0.32H, H–C(6 or 2) of η^6 -(*p*-cymene), *aa*), 5.37 (d, $^3J = 5.8$ Hz, 1H, H–C(2 or 6) of η^6 -(*p*-cymene), *as*), 5.21 (d, $^3J = 5.8$ Hz, 1H, H–C(5 or 3) of η^6 -(*p*-cymene), *as*), 4.34 (m, 1H, -CH-, *as*), 3.91 (m, 0.32H, -CH-, *aa*), 3.31–3.15 (3 partly res. dd, 1.64H, -CH₂-, *as* and *aa*), 2.86 (h, $^3J = 6.8$ Hz, 0.32H, -CH(CH₃)₂, *aa*), 2.67 (dd, $^2J = 13.8$, $^3J = 4.2$ Hz, 1H, -CH₂-, *as*), 2.54 (h, $^3J = 6.8$ Hz, 0.32H, -CH(CH₃)₂, *as*), 2.25 (s, 0.96H, -CH₃, *aa*), 2.13 (s, 3H, -CH₃, *as*), 1.31 (d, $^3J = 6.8$ Hz, 3H, -CH(CH₃)₂, *as*), 1.30 (d, $^3J = 6.8$ Hz, 0.96H, -CH(CH₃)₂, *aa*), 1.22 (d, $^3J = 6.8$ Hz, 0.96H, -CH(CH₃)₂, *aa*), 1.18 (d, $^3J = 6.8$ Hz, 3H, -CH(CH₃)₂, *as*). – ¹³C{¹H} NMR (CDCl₃, 75 MHz): $\delta = 136.67$ (C_{ipso} of *Ph-CH-*, *as* and *aa*), 133.05 (C_o of Ph-S-, *as*), 132.47 (C_p of Ph-S-, *as*), 131.42 (C_o of Ph-S-, *aa*), 131.32 (C_m of Ph-S-, *aa*), 130.89 (C_m of Ph-S-, *as*), 129.81 (C_m of *Ph-CH-*, *aa*), 129.60 (C_o of *Ph-CH-*, *as* and *aa*, C_m of *Ph-CH-*, *as*), 129.14 (C_p of Ph-S-, *aa*), 127.22 (C_p of *Ph-CH-*, *as*), 126.96 (C_p of *Ph-CH-*, *aa*), 108.76 (C(4) of η^6 -(*p*-cymene), *aa*), 106.13 (C(4) of η^6 -(*p*-cymene), *as*), 101.68 (C(1) of η^6 -(*p*-cymene), *as*), 101.28 (C(1) of η^6 -(*p*-cymene), *aa*), 87.84 (C(5 or 3) of η^6 -(*p*-cymene), *as*), 85.43 (C(2 or 6) of η^6 -(*p*-cymene), *as*), 85.26 (C(5 or 3) of η^6 -(*p*-cymene), *aa*), 84.80 (C(3 or 5) of η^6 -(*p*-cymene), *as*), 83.94 (C(6 or 2) of η^6 -(*p*-cymene), *aa*), 81.64 (C(6 or 2) of η^6 -(*p*-cymene), *as*), 60.37 (-CH-, *aa*), 60.22 (-CH-, *as*), 45.96 (-CH₂-, *as*), 43.54 (-CH₂-, *aa*), 31.18 (-CH(CH₃)₂, *as*), 30.98 (-CH(CH₃)₂, *aa*), 23.14 (-CH(CH₃)₂, *as*), 22.30 (-CH(CH₃)₂, *aa*), 22.14 (-CH(CH₃)₂, *as*), 21.90 (-CH(CH₃)₂, *aa*), 18.42 (-CH₃, *aa*), 18.15 (-CH₃, *as*). – FAB-MS: m/z (%) = 500 (100) [M – PF₆ – Cl]⁺ with respect to ¹⁰²Ru, 464 (18) [M – PF₆ – Cl]⁺ with respect to ¹⁰²Ru. – Anal. for C₂₄H₂₉ClF₆NPRuS(CH₂Cl₂)_{0.5}(H₃COH) (719.56): calcd. C 42.56, H 4.76, N 1.95, S 4.46; found C 42.46, H 4.45, N 2.00, S 4.60.

[(+)-(1'R)-Chloro- η^6 -[1,3,5-trimethylbenzene]- σ (N): σ (S)-[1'-phenyl-2'-(phenylthio)ethylamino]ruthenium(II)] hexafluorophosphate, [17][PF₆]

According to the above procedure, **15** (301 mg, 0.515 mmol) and **5** (254 mg, 1.107 mmol) were stirred for 13 h in MeOH (25 mL), and NaPF₆ (387 mg, 2.304 mmol) was added then. The soln. was stirred for 30 h and worked up as described above to afford 688 mg crude product as a solid yellow foam. The crude product was dissolved in a minimum

amount of warm CH₂Cl₂, layered at r.t. with MeOH and then with pentanes to be crystallized at –30 °C overnight: 523 mg (80 %) of [17][PF₆], yellow microcrystals (X-ray crystal structure analysis). After crystallization [17][PF₆] is only sparingly soluble in CHCl₃ or CH₂Cl₂, but moderately in acetone. – M. p. = 214–216 °C. – $[\alpha]_D^{23} = +20.8$ (CH₂Cl₂, $c = 0.00284$). – ¹H NMR (CDCl₃, 400 MHz, –30 °C; integration referenced to methyl singlet of the η^6 -mesitylene ligand assigned to the *as* diastereomer): $\delta = 7.96$, 7.90, 7.82 (3 pseudo d, 1.55H, H_o of Ph-S-), 7.68–7.30 (series of m, 13.36H, Ph-S-, *Ph-CH-*), 5.49 (s, 3H, η^6 -mesitylene, *as*), 5.44 (s, 1.20H, η^6 -mesitylene, *aa*), 5.36 (br s, -NH₂-), 5.24 (s, 0.30H, η^6 -mesitylene, *sa*), 5.19 (s, 0.21H, η^6 -mesitylene, *ss*), 5.08 (br s, -NH₂-), 4.72 (m, 0.55H, -CH-), 4.42 (m, 0.29H, -CH-), 4.25–4.10 (2 m, 1.07H, -CH-), 3.69 (m, 0.73H, -CH₂-), 3.54 (m, 1.31H, -CH₂-), 3.35 (m, 0.80H, -CH₂-), 3.12 (m, 1.07H, -CH₂-), 2.71 (dd, $^2J = 13.8$, $^3J = 3.8$ Hz, 0.30H, -CH₂-), 2.25 (s, 9H, -CH₃, *as*), 2.02 (s, 3.60H, -CH₃, *aa*), 1.87 (s, 0.63H, -CH₃, *ss*), 1.70 (s, 0.90H, -CH₃, *sa*). – ¹³C{¹H} NMR ([D₆]acetone, 75 MHz): $\delta = 139.18$ (C_{ipso} of Ph), 138.61 (C_{ipso} of Ph), 134.05 (C_{ipso} of Ph), 132.79–127.77 (Ph-S-, *Ph-CH-*), 105.86 (C_{ipso} of η^6 -mesitylene), 104.93 (C_{ipso} of η^6 -mesitylene), 82.52 (HC of η^6 -mesitylene), 81.77 (HC of η^6 -mesitylene); 81.45 (HC of η^6 -mesitylene), 62.17 (-CH-), 61.60 (-CH-), 60.15 (-CH₃), 46.79 (-CH₂-), 43.56 (-CH₂-), 39.55 (-CH₂-), 18.71 (-CH₃). – FAB-MS: m/z (%) = 486 (100) [M – PF₆ – Cl]⁺ with respect to ¹⁰²Ru, 450 (23) [M – PF₆ – Cl]⁺ with respect to ¹⁰²Ru, 331 (27) [M – PF₆ – Cl – C₉H₁₂]⁺ with respect to ¹⁰²Ru, 257 (24) [M – PF₆ – Cl – C₉H₁₂ – Ph]⁺ with respect to ¹⁰²Ru. – Anal. for C₂₃H₂₇ClF₆NPRuS (631.03): calcd. C 43.78, H 4.31, N 2.22, S 5.08; found C 43.84, H 4.59, N 2.21, S 5.03.

[(-)-(1'R)-Chloro- η^6 -[1,3,5-trimethylbenzene]- σ (N): σ (S)-[1'-phenyl-2'-(2''-naphthylthio)ethylamino]ruthenium(II)] hexafluorophosphate, [18][PF₆]

According to the above procedure **15** (302 mg, 0.517 mmol) and **7** (313 mg, 1.120 mmol) were stirred for 13 h in MeOH (25 mL), and NaPF₆ (392 mg, 2.334 mmol) was added then. The soln. was stirred for 30 h, worked up as described above and crystallized from CH₂Cl₂ layered with some drops of MeOH at –30 °C to afford 582 mg (83 %) of [18][PF₆] as yellow microcrystals (X-ray crystal structure analysis). Solubility of crystalline [18][PF₆]: acetone = MeCN > CH₂Cl₂ ≥ THF ≫ MeOH. – M. p. = 221–222 °C. – $[\alpha]_D^{23} = -8.6$ (CH₂Cl₂, $c = 0.00266$). – ¹H NMR ([D₆]acetone, 300 MHz, integration referenced to η^6 -mesitylene singlets assigned to the *aa* diastereomer): $\delta = 8.65$ –7.42 (series of m, 80.63H, β -Naph, Ph), 6.38 (br s, -NH₂-), 6.07 (not res. dd, 0.83H, -CH-), 5.81 (s, 2.92H, η^6 -mesitylene, *as*), 5.71 (s, 3H, η^6 -mesitylene, *aa*), 5.48 (2 br not res. s, 2.72H, η^6 -mesitylene, *sa* and *ss*), 5.34

(br s, -NH₂-), 4.64 (not res. dd, 0.53H, -CH-), 4.33–3.82 (2 not res. dd, 3.39H, -CH-, -CH₂-), 3.75 (dd, ²J = 32.9, ³J = 12.4 Hz, 2.10H, -CH₂-), 3.46–2.90 (series of m, 5.2H, -CH-, -CH₂-), 2.37 (s, 8.78H, -CH₃, *as*), 2.36 (s, 9H, -CH₃, *aa*), 2.18 (2 not res. s, 8.16H, -CH₃, *sa* and *aa*). – ¹³C{¹H} NMR ([D₆]acetone, 75 MHz): δ = 138.71 (*C*_{ipso} of Ph or C(2) of β -Naph), 138.17 (*C*_{ipso} of Ph or C(2) of β -Naph), 134.34–126.26 (β -Naph, Ph), 105.33 (*C*_{ipso} of η^6 -mesitylene), 104.28 (*C*_{ipso} of η^6 -mesitylene), 82.27 (HC of η^6 -mesitylene), 81.45 (HC of η^6 -mesitylene), 81.13 (HC of η^6 -mesitylene), 61.72 (-CH-), 61.06 (-CH-), 59.58 (-CH-), 50.20 (-CH₂-), 46.64 (-CH₂-), 43.11 (-CH₂-), 38.82 (-CH₂-), 31.98 (-CH₃), 31.47 (-CH₃), 20.15 (-CH₃). – FAB-MS: *m/z* (%) = 537 (100) [M – PF₆]⁺ with respect to ¹⁰²Ru, 501 (70) [M – PF₆ – Cl]⁺ with respect to ¹⁰²Ru. – Anal. for C₂₇H₃₀ClF₆NPRuS (682.09): calcd. C 47.54, H 4.43, N 2.05, S 4.70; found C 47.24, H 4.54, N 2.01, S 4.66.

[(+)-(*l*′ *R*)-Chloro- η^6 -[1,3,5-trimethylbenzene]- σ (N): σ (S)-[1′-phenyl-2′-(3′′-methylbut-2′′-enylthio)ethylamino]ruthenium(II)] hexafluorophosphate, [19][PF₆]

According to the above procedure **15** (411 mg, 0.703 mmol) and **13** (332 mg, 1.500 mmol) were stirred for 15 min in MeOH (6 mL), and NaPF₆ (361 mg, 2.149 mmol) was added then. The soln. was stirred for 16 h, worked up as described above and crystallized from a minimum amount of warm MeOH with some drops of CH₂Cl₂ by cooling from r. t. down to –30 °C overnight to afford 726 mg (78 %) of [19][PF₆]. The compound crystallizes with half a molecule of CH₂Cl₂ per formula unit (analytical data, X-ray structure analysis). – M. p. = 133–134 °C. – [α]_D²³ = +17.6 (CH₂Cl₂, *c* = 0.0017). – ¹H NMR (CDCl₃, 300 MHz, integration referenced to η^6 -mesitylene singlets assigned to the *aa* diastereomer): δ = 7.48–7.30 (m, 11.07H, Ph), 5.40 (s, 2.44H, η^6 -mesitylene, *as*), 5.36 (s, 3H, η^6 -mesitylene, *aa*), 5.28 (2 broadened s, 1.83H, η^6 -mesitylene, *sa* and *ss*), 5.27–5.19 (3 m, 1.93H, -CH=C(CH₃)₂), 5.16–4.96 (m, 1.93H, -CH-), 4.14–4.00 (m, 1.42H, -CH-), 3.78–3.34 (series of m, 8.70H, -CH-, -CH₂-), 3.08 (dd, ²J = ³J = 13.6 Hz, 1.17H, -CH₂-CH=C(CH₃)₂, *as* + *aa* or *sa* + *ss*), 2.83 (m, 0.92H, -CH₂-CH=C(CH₃)₂, *sa* + *ss* or *as* + *aa*), 2.67 (dd, ²J = 13.7, ³J = 11.3 Hz, 1.00H, -CH₂-CH=C(CH₃)₂, *sa* + *ss* or *as* + *aa*), 2.46–2.42 (m, 1.15H, -CH₂-CH=C(CH₃)₂, *as* + *aa* or *sa* + *ss*), 2.20 (s, 7.32H, -CH₃, *as*), 2.19 (s, 9H, -CH₃, *aa*), 1.81 and 1.75 (2 partly res. d, ⁴J_{cis} = 10.2 and ⁴J_{trans} = 16.1 Hz, 11.81H, -CH₂-CH=C(CH₃)₂, all diastereomers), 1.39 (s, 0.48H, -CH₃, *ss*), 1.09 (s, 1.36H, -CH₃, *sa*). – ¹³C{¹H} NMR (CDCl₃, 75 MHz): δ = 141.77 (*C*_{ipso} of Ph), 141.65 (*C*_{ipso} of Ph), 137.68 (*C*_{ipso} of Ph), 136.37 (-CH=C(CH₃)₂), 129.63 (*C*_p of Ph), 129.54 (*C*_m of Ph), 129.43 (*C*_p of Ph), 127.16 (*C*_o of Ph), 126.89 (*C*_o of Ph), 115.82 (-CH=C(CH₃)₂), 115.76 (-CH=C(CH₃)₂), 105.21 (HC of η^6 -mesitylene), 103.77 (HC of η^6 -mesitylene), 81.07

(*C*_{ipso} of η^6 -mesitylene, *sa*), 80.35 (HC of η^6 -mesitylene, *aa*), 62.61 (-CH-), 60.78 (-CH-), 59.76 (-CH₃, *ss*), 40.46 (-CH₂-CH=C(CH₃)₂, *as* + *aa* or *sa* + *ss*), 38.13 (-CH₂-CH=C(CH₃)₂, *sa* + *ss* or *as* + *aa*), 36.86 (-CH₂-), 35.46 (-CH₂-), 31.79 (-CH₂-), 31.22 (-CH₃, *sa*), 25.90 (-CH₂-CH=C(CH₃_{cis})(CH₃)), 18.51 (-CH₂-CH=C(CH₃)(CH₃_{trans}), -CH₃, *as* + *aa*). – FAB-MS: *m/z* (%) = 479 (100) [M – PF₆]⁺ with respect to ¹⁰²Ru, 374 (38) [M – PF₆ – Cl – Prn]⁺ with respect to ¹⁰²Ru, 254 (22) [M – PF₆ – Cl – Prn – mesitylene]⁺ with respect to ¹⁰²Ru. – Anal. for C₂₂H₃₁ClF₆NPRuS (CH₂Cl₂)_{0.5} (665.51): calcd. C 40.61, H 4.85, N 2.10, S 4.82; found C 40.59, H 4.88, N 2.08, S 4.81.

Crystal structure determinations

Crystal parameters, data collection and structure refinement details are summarized in Table 11. Intensity data were collected at 100 K on a Bruker-Nonius KappaCCD diffractometer (MoK α radiation, λ = 0.71073 Å, graphite monochromator). Absorption corrections were performed using either a numerical Gauss integration [11a] or on the basis of multiple scans with SADABS [11b]. All structures were solved with Direct Methods and refined by full-matrix least-squares procedures on *F*² [12]. The absolute configurations were confirmed, respectively determined, by anomalous dispersion effects by means of Flack's *x* refinement [13]. All non-hydrogen atoms were refined with anisotropic displacement parameters. All H-atoms were placed in positions of optimized geometry; their isotropic displacement parameters were tied to the equivalent isotropic displacement parameters of their corresponding carrier atoms by a factor of 1.2 or 1.5, respectively. The CH₂Cl₂ solvent molecule in the crystal structure of [16][PF₆] is situated on a crystallographic twofold axis. High anisotropic displacement parameters for some carbon atoms in the crystal structure of [17][PF₆] indicate a possible disorder. However, attempts to resolve this disorder remained unsuccessful. Similarity restraints (SIMU) were applied in the refinement of some of the carbon atoms in the crystal structure of [18][PF₆]. The PF₆[–] anions in the crystal structure of [19][PF₆] are located on crystallographic twofold axes. The CH₂Cl₂ solvent molecule in [19][PF₆] is disordered.

CCDC 669750 (**9**), CCDC 669751 ([16][PF₆]·(CH₂Cl₂)_{0.5}·(MeOH)), CCDC 669752 ([17][PF₆]), CCDC 669753 ([18][PF₆]) and CCDC 669754 ([18][PF₆]·(CH₂Cl₂)_{0.5}) contain the supplementary crystallographic data for this paper. These data can be obtained free of charge from the Cambridge Crystallographic Data Centre via http://www.ccdc.cam.ac.uk/data_request/cif.

Acknowledgements

We are grateful to the Deutsche Forschungsgemeinschaft (SFB 583) for financial support and to the fol-

lowing colleagues of the Department Chemie & Pharmazie, Friedrich-Alexander-Universität Erlangen-Nürnberg: Prof. Dr. Peter Gmeiner (Emil Fischer Center) and Prof. Dr. Andreas Hirsch (Organic Chemistry and Interdis-

ciplinary Center for Molecular Materials (ICMM)) for providing access to essential analytical equipment, and Dr. Wolfgang Utz (Emil Fischer Center) for helpful discussions.

- [1] a) K. Mashima, H. Kaneyoshi, S.-I. Kaneko, A. Mikami, K. Tani, A. Nakamura, *Organometallics* **1997**, *16*, 1016–1025; b) K. Mashima, S.-I. Kaneko, K. Tani, H. Kaneyoshi, A. Nakamura, *J. Organometal. Chem.* **1997**, *545–546*, 345–356; c) F. Chérioux, C. M. Thomas, T. Monnier, G. Süss-Fink, *Polyhedron* **2003**, *22*, 543–548; d) F. Chérioux, B. Therrien, G. Süss-Fink, *Chem. Commun.* **2004**, 204–205; e) M. Tschan, B. Therrien, F. Chérioux, G. Süss-Fink, *J. Mol. Struct.* **2005**, *743*, 177–181; f) F. Chérioux, B. Therrien, G. Süss-Fink, *Inorg. Chim. Acta* **2004**, *357*, 834–838; g) J. Cubrilo, I. Hartenbach, F. Lissner, T. Schleid, M. Niemeyer, R. F. Winter, *J. Organomet. Chem.* **2007**, *692*, 1496–1504; h) D. P. Halbach, C. G. Hamaker, *J. Organometal. Chem.* **2006**, *691*, 3349–3361; *Inorg. Chim. Acta* **2006**, *359*, 846–852; i) M. A. Bennett, L. Y. Goh, A. C. Willis, *J. Chem. Soc., Chem. Commun.* **1992**, 1180–1182; j) M. A. Bennett, L. Y. Goh, A. C. Willis, *J. Am. Chem. Soc.* **1996**, *118*, 4984–4992; k) R. Y. C. Shin, M. A. Bennett, L. Y. Goh, W. Chen, D. C. R. Hockless, W. K. Leong, K. Mashima, A. C. Willis, *Inorg. Chem.* **2003**, *42*, 96–106; l) R. Y. C. Shin, L. Y. Goh, *Acc. Chem. Res.* **2006**, *39*, 301–313; m) J. G. Planas, C. Viñas, F. Teixidor, M. E. Light, M. B. Hursthouse, H. R. Ogilvie, *Eur. J. Inorg. Chem.* **2005**, 4193–4205; n) D.-H. Wu, C. Ji, Y.-Z. Li, H. Yan, *Organometallics* **2007**, *26*, 1560–1562.
- [2] a) H. Brunner, G. Riepl, H. Weitzer, *Angew. Chem.* **1983**, *95*, 326; *Angew. Chem., Int. Ed. Engl.* **1983**, *22*, 331; b) H. Brunner, R. Becker, G. Riepl, *Organometallics* **1984**, *3*, 1354–1359; c) R. P. Hof, M. A. Poelert, N. C. M. W. Peper, R. M. Kellogg, *Tetrahedron: Asymmetry* **1994**, *5*, 31–34; d) J. Kang, D. S. Kim, J. I. Kim, *Synlett* **1994**, 842–844; e) F. Leyendecker, D. Laucher, *Tetrahedron Lett.* **1983**, *24*, 3517–3522; f) R. K. Dieter, M. Tokles, *J. Am. Chem. Soc.* **1987**, *109*, 2040–2046; g) V. T. Myllymäki, M. K. Lindvall, A. M. P. Koskinen, *Tetrahedron* **2001**, *57*, 4629–4635; h) E. W. Abel, A. Kahn, K. Kite, K. G. Orrell, V. Šik, *J. Organomet. Chem.* **1978**, *145*, C18–C20; i) J. Eekhof, H. Hogeveen, R. M. Kellogg, E. Klei, *J. Organomet. Chem.* **1978**, *161*, 183–195; j) G. Tresoldi, L. Baradello, S. Lanza, P. Cardiano, *Eur. J. Inorg. Chem.* **2005**, 2423–2435.
- [3] a) H.-U. Blaser, C. Malan, B. Pugin, F. Spindler, H. Steiner, M. Studer, *Adv. Synth. Catal.* **2003**, *345*, 103–151, and refs. therein; b) R. Noyori, T. Okhuma, *Angew. Chem.* **2001**, *113*, 40–75; *Angew. Chem. Int. Ed.* **2001**, *40*, 40–73, and refs. therein; c) S. Hashiguchi, A. Fujii, J. Takehara, T. Ikariya, R. Noyori, *J. Am. Chem. Soc.* **1995**, *117*, 7562–7563; d) K.-J. Haack, S. Hashiguchi, A. Fujii, T. Ikariya, R. Noyori, *Angew. Chem.* **1997**, *109*, 297–300; *Angew. Chem., Int. Ed. Engl.* **1997**, *36*, 285–288; e) K.-J. Haack, S. Hashiguchi, A. Fujii, T. Ikariya, R. Noyori, *Angew. Chem.* **1997**, *109*, 300–303; *Angew. Chem., Int. Ed. Engl.* **1997**, *36*, 288–290; f) M. Yamakawa, I. Yamada, R. Noyori, *Angew. Chem.* **2001**, *113*, 2900–2903; *Angew. Chem. Int. Ed.* **2001**, *40*, 2818–2821; g) M. Yamakawa, H. Ito, R. Noyori, *J. Am. Chem. Soc.* **2000**, *122*, 1466–1478; h) A. Fujii, S. Hashiguchi, N. Uematsu, T. Ikariya, R. Noyori, *J. Am. Chem. Soc.* **1996**, *118*, 2521–2522; i) M. J. Palmer, M. Wills, *Tetrahedron: Asymmetry* **1999**, *10*, 2045–2061, and refs. therein; j) J.-B. Sortuis, V. Ritleng, A. Voelklin, A. Moluige, H. Smail, L. Barloy, C. Sirlin, G. K. M. Verzijl, J. A. F. Boogers, A. H. M. de Vries, J. G. de Vries, M. Pfeffer, *Org. Lett.* **2005**, *7*, 1247–1250; g) J. W. Faller, P. P. Fontaine, *J. Organometal. Chem.* **2007**, *692*, 976–982.
- [4] a) I. Weber, F. W. Heinemann, W. Bauer, S. Superci, A. Zahl, D. Richter, U. Zenneck, *Organometallics* **2008**, *27*, 4116–4152; b) P. Pinto, A. W. Götz, B. A. Hess, A. Marinetti, F. W. Heinemann, G. Marconi, U. Zenneck, *Organometallics* **2006**, *25*, 2607–2616; c) P. Pinto, G. Marconi, F. W. Heinemann, U. Zenneck, *Organometallics* **2004**, *23*, 374–380; e) G. Marconi, H. Baier, F. W. Heinemann, P. Pinto, H. Pritzkow, U. Zenneck, *Inorg. Chim. Acta* **2003**, *352*, 188–200.
- [5] a) F. Leyendecker, D. Laucher, *Nouv. J. Chim.* **1985**, *9*, 13–19; b) I. W. Davies, T. Gallagher, R. B. Lamont, D. I. C. Scopes, *J. Chem. Soc., Chem. Commun.* **1992**, 355–357; c) S. Takano, H. Iida, K. Inomata, K. Ogasawara, *Heterocycles* **1993**, *35*, 47–52; d) K. Matsuo, T. Arase, *Chem. Pharm. Bull.* **1995**, *43*, 2091–2094; e) B. G. Donner, *Tetrahedron Lett.* **1995**, *36*, 1223–1226; f) C. L. Gibson, *Tetrahedron: Asymmetry* **1996**, *7*, 3357–3358; g) T. Shinohara, J. Toda, T. Sano, *Chem. Pharm. Bull.* **1997**, *45*, 813–819; h) T. Shinohara, A. Takeda, J. Toda, N. Teresawa, T. Sano, *Heterocycles* **1997**, *46*, 555–566; i) H. Ishibashi, K. Ohata, M. Niihara, T. Sato, M. Ikeda, *J. Chem. Soc., Perkin Trans. I* **2000**, 547–553; j) L. I. Tank, *Med. Radiol.* **1961**, *6*, 76–77; k) G. H. Krongerg, R. S. Leard, B. H. Takman, *J. Med. Chem.* **1973**, *16*, 739–743;

- l) H. Tucker, J. F. Cope, *J. Med. Chem.* **1978**, *21*, 769–773; m) H. H. Herman, P. A. Husain, J. E. Colbert, M. M. Schweri, S. H. Pollock, L. C. Fowler, S. W. May, *J. Med. Chem.* **1991**, *34*, 1082–1085; n) J. M. Tomkins, K. J. Barnes, A. J. Blacker, W. J. Watkins, C. Abell, *Tetrahedron Lett.* **1997**, *38*, 691–694.
- [6] a) M. J. McKennon, A. I. Meyers, K. Drauz, M. Schwarm, *J. Org. Chem.* **1993**, *58*, 3568–3571; b) C. Marinzi, S. J. Bark, J. Offer, P. E. Dawson, *Bioorg. Med. Chem.* **2001**, *9*, 2323–23228; c) J. D. Dunitz, *X-Ray Analysis and the Structure of Organic Molecules*, Cornell University Press, Ithaca, **1979**; d) K. N. Houk, M. N. Paddon-Row, N. G. Rondan, Y.-D. Wu, F. K. Brown, D. C. Spellmeyer, J. T. Metz, Y. Li, R. J. Loncharich, *Science* **1986**, *231*, 1108.
- [7] a) L. N. Pridgen, J. Prol, Jr., *J. Org. Chem.* **1989**, *54*, 3231–3233; b) S. G. Davies, M. E. C. Polywka, H. J. Sanganee, U. S 005801249A, **1998** (assigned to Oxford Asymmetry International plc.); c) H. Ishibashi, M. Uegaki, M. Sakai, Y. Takeda, *Tetrahedron* **2001**, *57*, 2115–2120; d) H. Ishibashi, M. Uegaki, M. Sakai, *Synlett* **1997**, 915–916; e) A. Bewick, J. M. Mellor, W. M. Owton, *J. Chem. Soc., Perkin Trans. 1* **1985**, 1039–1044; f) M.-C. Fournié-Zaluski, P. Coric, S. Turcaud, L. Bruetschy, E. Lucas, F. Noble, B. P. Roques, *J. Med. Chem.* **1992**, *35*, 1259–1266; g) Y. Isamu, J. P 57193447, **1982** (assigned to Mitsui Toatsu Kagaku KK).
- [8] a) M. A. Bennett, G. Robertson, A. K. Smith, *J. Chem. Soc., Dalton Trans.* **1974**, 233–241; b) M. A. Bennett, T.-N. Huang, T. W. Matheson, A. K. Smith, *Inorg. Synth.* **1982**, *21*, 74–78; c) A. H. A. van der Zeijden, J. Jimenez, C. Mattheis, C. Wagner, K. Merzweiler, *Eur. J. Inorg. Chem.* **1999**, 1919–1930.
- [9] U. Bünzli-Trepp, *Handbuch für die systematische Nomenklatur der Organischen Chemie, Metallorganischen Chemie und Koordinationschemie*, Part A 6.4(d), Logos Verlag, Berlin, **2001**.
- [10] a) H. Brunner, R. G. Gastinger, *J. Organomet. Chem.* **1978**, *145*, 365–373; b) R. D. Peacock, B. Stewart, *Coord. Chem. Rev.* **1982**, *46*, 129–157; c) M. Ziegler, A. von Zelewsky, *Coord. Chem. Rev.* **1998**, *177*, 257–300; d) H. E. Smith, *Chem. Rev.* **1998**, *98*, 1709–1740; e) W. C. Johnson, Jr., L. P. Fontana, H. E. Smith, *J. Am. Chem. Soc.* **1987**, *109*, 3361–3366.
- [11] a) P. Coppens in *Crystallographic Computing*, (Eds.: F. R. Ahmed, S. R. Hall, C. P. Huber), Munksgaard, Copenhagen, **1970**, pp. 255–270; b) G. M. Sheldrick, SADABS (version 2.03), Program for Empirical Absorption Correction of Area Detector Data, University of Göttingen, Göttingen (Germany) **2002**.
- [12] a) COLLECT, Program for Data Collection, Bruker-Nonius, Karlsruhe (Germany) and Delft (The Netherlands) **2002**; b) EvalCCD, Program for Data Reduction; Bruker-Nonius, Karlsruhe (Germany) and Delft (The Netherlands) **2002**; c) G. M. Sheldrick, SHELXTL (version 6.12), Bruker AXS Inc., Madison, Wisconsin (USA) **2002**.
- [13] a) H. D. Flack, *Acta Cryst.* **1983**, *A39*, 876–881; b) A. J. C. Wilson (Ed.), *International Tables for Crystallography*, Vol. C, Kluwer Academic Publishers, Dordrecht **1992**, Table 6.1.1.4, pp. 500–502; Table 4.2.6.8, pp. 219–222; Table 4.2.4.2, pp. 193–199.